FINAL REPORT

Ultra-High Efficiency / Low Hydrogen Embrittlement Nanostructured ZN-Based Electrodeposits as Environmentally Benign CD-Replacement Coatings for High Strength Steel Fasteners

SERDP Project WP-1616

APRIL 2011

Jonathan McCrea
Integran Technologies, Inc.

SERDP
DOD • EPA • DOE

REPORT DOCUMENTATION PAGE

Form Approved
OMB No. 0704-0188

1. REPORT DATE *(DD-MM-YYYY)* 30-04-2011	2. REPORT TYPE FINAL	3. DATES COVERED *(From - To)* 04-08-2008 to 30-04-2011

4. TITLE AND SUBTITLE
Ultra-High Efficiency / Low Hydrogen Embrittlement Nanostructured Zn-Based Electrodeposits as Environmentally Benign Cd-Replacement Coatings for High Strength Steel Fasteners

5a. CONTRACT NUMBER

5b. GRANT NUMBER

5c. PROGRAM ELEMENT NUMBER

6. AUTHOR(S)
Jonathan McCrea, Brandon Bouwhuis

5d. PROJECT NUMBER
WP-1616

5e. TASK NUMBER

5f. WORK UNIT NUMBER

7. PERFORMING ORGANIZATION NAME(S) AND ADDRESS(ES)
Integran Technologies Inc.
6300 Northam Drive
Mississauga, Ontario
Canada L4V 1H7

8. PERFORMING ORGANIZATION REPORT NUMBER

9. SPONSORING / MONITORING AGENCY NAME(S) AND ADDRESS(ES)
Strategic Environmental Research and Development Program
901 North Stuart Street, Suite 303 Arlington, VA 22203

10. SPONSOR/MONITOR'S ACRONYM(S)
SERDP

11. SPONSOR/MONITOR'S REPORT NUMBER(S)

12. DISTRIBUTION / AVAILABILITY STATEMENT

13. SUPPLEMENTARY NOTES

14. ABSTRACT
The objective of SERDP project WP-1616 was to develop, and investigate the benefit of, nanostructured Zn-based alloys over current (Cd) and emerging (LHE ZnNi) sacrificial protective coatings, focusing in particular on the relevant properties for high strength steel fasteners. In Phase I, a number of nanostructured zinc (Zn)-based alloy coatings were successfully synthesized (Zn-Co, Zn-Fe, Zn-Ni and Zn-Ni-Co, in particular) based on simple modifications to currently available (off-the-shelf) commercial bath chemistries. The various nanostructured Zn-alloys were then subjected to comprehensive characterization and performance tests, including: grain size, crystallographic texture, microhardness, ductility, torque/tension friction, salt-spray corrosion and hydrogen embrittlement performance. Based on the Phase I results, the alkaline Zn-Ni, acid Zn-Ni and acid Zn-Ni-Co plating systems where selected as the most promising alloys to carry forward for further optimization in Phase II. The results in this report show that Integran's waveform engineering approach provides additional benefit over conventional DC plating and can be successfully integrated into a commercial scale as a potential swap-out technology with current Cadmium-plating.

15. SUBJECT TERMS
Nanocrystalline, Nanostructured, Sacrificial corrosion, Cadmium replacement, Hydrogen Embrittlement, Hydrogen Re-embrittlement, Salt Spray, Zinc, Nickel

16. SECURITY CLASSIFICATION OF:			17. LIMITATION OF ABSTRACT	18. NUMBER OF PAGES	19a. NAME OF RESPONSIBLE PERSON Jonathan McCrea
a. REPORT	b. ABSTRACT	c. THIS PAGE			19b. TELEPHONE NUMBER *(include area code)* 416-675-6266 x235

Standard Form 298 (Rev. 8-98)
Prescribed by ANSI Std. Z39.18

EXECUTIVE SUMMARY

The objective of SERDP project WP-1616 was to develop, and investigate the benefit of, nanostructured Zn-based alloys over current (Cd) and emerging (LHE ZnNi) sacrificial protective coatings, focusing in particular on the relevant properties for high strength steel fasteners. In Phase I, a number of nanostructured zinc (Zn)-based alloy coatings were successfully synthesized (Zn-Co, Zn-Fe, Zn-Ni and Zn-Ni-Co, in particular) based on simple modifications to currently available (off-the-shelf) commercial bath chemistries. The various nanostructured Zn-alloys were then subjected to comprehensive characterization and performance tests, including: grain size, crystallographic texture, microhardness, ductility, torque/tension friction, salt-spray corrosion and hydrogen embrittlement performance. Based on the Phase I results, the alkaline Zn-Ni, acid Zn-Ni and acid Zn-Ni-Co plating systems where selected as the most promising alloys to carry forward for further development in Phase II.

Upon completion of Phase I, the fine grained structures produced via pulse plating from modified commercial Zn-alloy plating solutions were found to have a number of significant benefits over conventional DC plating, including:

1) bright, uniform, dense microstructure,
2) uniform, equiaxed grain size throughout the thickness of the coating,
3) increased microhardness,
4) single γ-phase crystallographic microstructure (in the case of Zn-Ni),
5) increased corrosion resistance compared to other Zn-Ni alloys,
6) decreased friction (torque-tension), and
7) passing the ASTM F519 hydrogen embrittlement (HE) test (even with a dense microstructure, i.e. without porosity).

The benefits of pulse plating on the performance of Zn-alloys are expected to provide superior coating properties similar or superior to Cd and essential to high strength steel fasteners.

Phase II was carried out in five additional tasks: (1) optimization of a selected nanocrystalline Zn-based alloy; (2) evaluation of trivalent (Cr^{3+}) and hexavalent chromium (Cr^{6+}) conversion coatings to enhance corrosion resistance; (3) test sample production for the testing of hydrogen re-embrittlement (HRE) (a.k.a. in-service embrittlement); (4) further optimization of plating conditions specific for fasteners; and (5) evaluation of scaled-up production plating, focusing particularly on bath stability and barrel plating.

The main conclusions from Phase II were as follows:
- ZnNi coatings synthesized from alkaline bath chemistries had greater compositional uniformity (less fluctuation with variations in current density) compared to those from acid chemistries, resulting in more uniform peak to valley composition in threaded fasteners.
- In addition to providing dense structures, pulse plated deposits typically possessed higher nickel content than direct current (DC) plated deposits from the same plating bath.
- Both the hexavalent chromate conversion coating and trivalent chromium conversion coating were successfully applied to the pulse plated ZnNi structures, providing similar enhancement to salt spray corrosion performance.
- The ability to pass the hydrogen re-embrittlement test (pass defined as four samples lasting longer than 150hrs when loaded to 45% of the notch fracture strength of ASTM F519 Type 1a1 bars) highly depends on the following factors:
  o *Pre-plating treatment methods*: samples activated with acid activation had significantly decreased time to failure in the re-embrittlement test, even though the samples passed regular ASTM F519 testing,

- o *Porosity of coating*: dense, non-porous ZnNi coatings routinely outperformed porous ZnNi structures,
  - o *Nickel content*: Time to failure in the re-embrittlement test was significantly dependent on the nickel concentration in the deposit (i.e. a pulse plated sample with 15wt.%Ni passed 150hrs while the same with a 12wt.%Ni content failed in less than 2hrs).
  - o *The open circuit potential (OCP)*: The OCP was found to be highly dependent on the nickel content in the 12-15wt.%Ni range. This could help explain the HRE performance as a nickel concentration of 15wt.% had an OCP close to that of Cd and steel, which would create less of a galvanic potential when coupled with steel.
- Bulk processing of a large numbers of fasteners was successfully accomplished using pulsed electrical parameters while barrel plating.

The results obtained demonstrate that dense, fine grained Zn-alloy structures synthesized via pulse electrodeposition using a commercial Zn-Ni alkaline system supplied by Dipsol of America can lead to the retention of numerous benefits associated with Cadmium-coating technology, including: non-line-of-sight application, excellent corrosion resistance, low coefficient of friction, excellent coating adhesion, high dimensional consistency and superior surface finish. The use of pulse plating was also found to have benefits over conventional ZnNi plating, including superior corrosion protection and improved HRE performance as a result of the dense fine grained microstructure. Furthermore, pulse electrodeposition can be implemented within the existing Cadmium-plating infrastructure within the defense sector for conventional rack plating as well as bulk plating of fasteners, e.g. barrel plating.

TABLE OF CONTENTS

LIST OF FIGURES

vi

LIST OF TABLES

LIST OF ACRONYMS

A	Amperes
ASTM	American Society for Testing and Materials
AMS	American Measurement Standard
Cd	Cadmium
Co	Cobalt
Cr	Chromium
DC	Direct Current
Dem/Val	Demonstration / Validation
DoE	Design of Experiments
EDX/EDS	Energy-Dispersive X-Ray Spectroscopy
EPA	Environmental Protection Agency
ESTCP	Environmental Security Technology Certification Program
Fe	Iron
HSS JTP	High-Strength Steel Joint Test Protocol
HE	Hydrogen Embrittlement
HRE	Hydrogen Re-Embrittlement / In-Service Embrittlement
HSS	High-Strength Steel
Hz	Hertz
IVD	Ion-Vapour Deposition
IR	Infrared
JCAT	Joint Cadmium Alternative Team
LHE	Low Hydrogen Embrittlement
m	Meters
MS	Mild Steel
min.	Minutes
μm	Microns, 10^{-6} meters
NFS	Notch Fracture Strength
NH_4Cl	Ammonium Chloride
Ni	Nickel
nm	Nanometers, 10^{-9} meters
PP	Pulse-Plating
ppm	Parts Per Million
PR	Pulse-Reverse Plating
SAE	Society of Automotive Engineers
SEM	Scanning Electron Microscopy
SERDP	Strategic Environmental Research and Development Program
Sol-Gel	Chemical Solution Deposition Process
TDS	Technical Data Sheet
UNC	Universal Naming Convention
V	Volts
VHN	Vickers Hardness Number, also kg/mm^2
XRD	X-Ray Diffraction
XRF	X-Ray Fluorescence
Zn	Zinc

ACKNOWLEDGEMENTS

1.0 INTRODUCTION

1.1 CADMIUM (CD) PLATING TECHNOLOGY

For steel fasteners used in the aerospace and transportation industries, Cadmium (Cd) coatings are the choice of most major manufacturers due to its superior corrosion resistance, lubricity, and fatigue resistance. When electroplated onto steel fasteners and parts, Cd provides cathodic protection in the form of an impermeable sacrificial coating due to its lower position on the galvanic scale compared to low alloy steel [1]. High lubricity allows Cd coated fasteners to be repetitively installed and reduces the torque required for tightening [1]. Resistance to fatigue extends the life of the plated fastener which, combined with the corrosion resistance and ability to re-install, results in a long-lasting reliable product. Electrodeposition is the most common method of coating high strength steel fasteners with Cd. Typically Cd is post-treated with chromium conversion coatings to increase the durability of the part before installation [1].

The Environmental Protection Agency (EPA) has indicated that Cd is a class B1 carcinogen resulting from both inhalation and ingestion. It has been banned from most industries due to its tendency to reside in body tissue [2,3]. Cd electroplating produces toxic fumes which affect bath operators [2]. Cd waste disposal and emissions are heavily regulated in most countries to attempt to avoid contamination of food and water sources [2]. Risks are not limited to those created in plating shops as Cd dissolves in rainwater, thus extending the danger of exposure throughout the entire life of the coated part, from plating, to installation and usage and finally disposal [3].

1.2 EXISTING CD-REPLACEMENT ALTERNATIVES

As a result of the strict regulation of Cd-containing processes, there are significant ongoing efforts to develop effective Cd-replacement technologies. The most promising concepts (such as ion-vapour deposited (IVD) aluminum, AlumiPlate™, standard electrodeposited acid and alkaline zinc nickel (Zn-Ni) and metallic ceramics) have, to some extent, found acceptance in various military and commercial Cd-replacement roles. In general, these replacement technologies can be grouped into two classes, 'wet' (i.e. electrodeposition) or 'dry' techniques. 'Dry' techniques include physical or chemical vapour deposition methods, such as IVD aluminum. However, when tested, IVD aluminum coatings displayed poor adhesion and possible susceptibility to corrosion [4]. This may be due to the fact that pure aluminum coatings have insufficient corrosion resistance, and thus a chromate or chromium conversion coating must be used to enhance surface properties [3]. Aluminum-molybdenum unbalanced magnetron sputter deposition is another alternative technology. Aluminum-rich coatings can be used for corrosion resistance and adhesion, and molybdenum rich coatings can provide the lubricity required to replace Cd on high strength steel fasteners [3]. However, these 'dry' technologies are expensive, require significant investment on the industry's behalf and work on line-of-sight applications only.

Cadmium alternative programs are also being implemented by the Joint Cadmium Alternative Team (JCAT) [e.g. 5] and the Environmental Security Technology Certification Program (ESTCP) [e.g. 6]. The leading 'wet' Cd-replacement technology is Zn-Ni electrodeposition, not least because it provides a logical fit to replace industrial Cd electroplating processes. Indeed, Zn-Ni plating has been gaining significant momentum as a suitable drop-in alternative, especially in the commercial aerospace industry. Acid-based Zn-Ni is qualified for use as a Cd-replacement alternative. However, it is not an operator friendly process and is only applicable to low strength steels (< 160 ksi) [7]. The established Zn-Ni plating processes are not 100% efficient, which means that hydrogen will be a by-product of the desired metal reduction reactions during plating. This hydrogen evolution is thought to be the cause of hydrogen embrittlement (HE) of the steel substrate [3]. Low and medium-strength steels are not susceptible to HE while high-strength steels are. The Boeing Company, in partnership with Dipsol of America, has developed a Low Hydrogen Embrittlement (LHE) Alkaline Zn-Ni process (IZ-C17) specifically for

application to high strength steel [8,9,10]. The LHE Alkaline Zn-Ni process eliminates the use of brighteners to create a dull, porous coating, and currently shows promising results in regards to corrosion, hydrogen embrittlement (HE), and in-service hydrogen re-embrittlement (HRE) [8,9,10,11]. In particular, through qualification testing [e.g. 7,12] it has been shown that the LHE IZ-C17 system performs in many ways as well as cadmium [10]. However, the process is not yet optimized [10,]: for example, the LHE C-17 coating is considered brittle and requires improved lubricity; HRE testing has been completed primarily using the incremental step load method [e.g. 11]; application of brush plating is questionable [e.g. 11]; and the composition plays a large role in the overall performance.

If an acceptable level of hydrogen transfer can be achieved by creating a coating structure that is <u>highly diffusive to hydrogen while remaining relatively smooth and non-porous,</u> then it is likely that the proven corrosion-resistant capability of Zn-based coatings can be maintained and not compromised. Moreover, if this can be done with a process that is close to 100% cathodic current efficiency (i.e. produces less hydrogen), then the probability of embrittlement of the high strength substrate will be diminished even further.

1.3   SYNTHESIS, STRUCTURE & PROPERTIES OF ELECTRODEPOSITED NANOSCALE MATERIALS

Integran Technologies produces nanoscale metallic coatings for various applications and has been actively investigating Cd replacement by evaluating possible alternative coatings. Integran takes advantage of the existing infrastructure of electrodeposition and achieves nanostructured materials to meet many customer requests through customized bath chemistry and applied electrical parameters. By reducing grain size of the electrodeposited metal to the nanoscale, deposits with superior mechanical properties are produced. These improved mechanical properties, such as hardness, corrosion resistance, tensile strength, and low coefficient of friction, would be valuable for a coating applied to high strength steel fasteners.

Electrodeposited nanostructures have advanced rapidly to commercial application as a result of: 1) an established industrial infrastructure (i.e., electroplating and electroforming industries), 2) a relatively low cost of application whereby nanomaterials can be produced by simple modification of bath chemistries and electrical parameters used in current plating and electroforming operations, and 3) the capability in a single-step process to produce metals, alloys, and metal-matrix composites in various forms (i.e., coatings, free-standing complex shapes). The earliest systematic studies on the use of electrodeposition to produce nanocrystalline materials (i.e. materials with grain size values below 100 nm) were published in the late 1980's by the present applicants and the general conditions for producing nanocrystalline metals and alloys by electrodeposition are documented in US Patent No. 5,352,266 (Oct. 4, 1994) and US Patent No. 5,433,797 (July 18, 1995). The nanocrystalline materials synthesized in this project were fabricated following the methods and covered by various US and international patents [13,14,15,16,17,18,19]. SERDP has been instrumental in the advancement of electrodeposited nanostructures through its previous support of Integran in the development of a nanoscale Co-based hard chrome replacement technology (SERDP WP-1152), which has successfully advanced to the Dem/Val stage with a demonstration tank installation at NADEP-JAX (ESTCP WP-0411).

Integran optimizes electrodeposited nanostructured materials through a variety of methods, including utilizing different electrical parameters. Altering electrical parameters includes the application of various current densities (mA/cm^2) and pulse timings. Pulse timings can refer to varying the applied frequency, forward to reverse current ratios, and current on and off times. Three employed pulse timings are direct current (DC), pulse plating (PP), and pulse reverse (PR) plating (Figure 1). DC is the application of a constant forward current and is the most common waveform applied in industry. PP occurs when a forward current is applied and turned off regularly. This approach results in a more fine-grained, defect-free, and compositionally-uniform deposit due to the replenishment of the plating solution at the cathode surface during the time-off portion of the cycle [20]. PR plating is the application of a cathodic pulse

followed by an anodic pulse. By applying reverse current, the coating is selectively removed from areas of the part that have preferentially grown quicker, which allows for a more level and fine-grained deposit that is typically low in deformities [20]. By changing the applied waveform, it is possible to alter the properties and characteristics of the deposit.
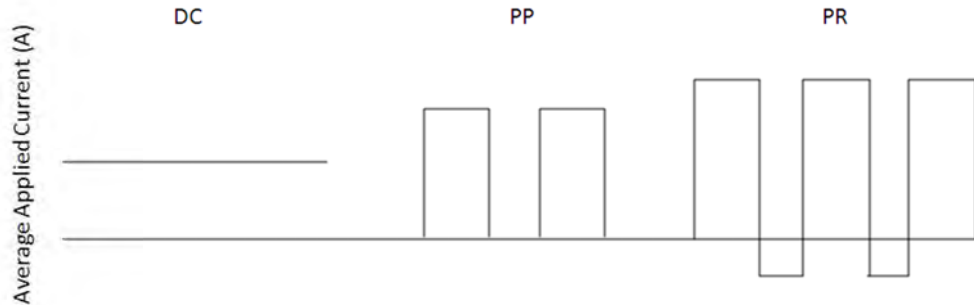
Figure 1: Depictions of direct current (DC), pulse (PP), and pulse reverse (PR) waveforms.

1.3.1 Hydrogen Embrittlement (HE) and Re-Embrittlement (HRE)

Studies [21,22] into the transport behavior of hydrogen in nickel (Ni) as determined by an electrolytic charging technique revealed that substantial increases in hydrogen diffusivity and capacity are obtained when Ni is in the nanocrystalline form. Figure 2 illustrates three representative permeation transients corresponding to hydrogen transport through nanocrystalline (20 nm), fine grained (1 µm), and single crystalline Ni foils of 140 µm thickness. Detection of permeated hydrogen in the Ni bi-electrodes of identical thickness is observed in the following order: 1) nanocrystalline, 2) fine grained, 3) single crystal structures. In this study, the hydrogen diffusivity of the nanocrystalline material was calculated to be approximately 100× greater than that of the same metal in coarse-grained form. In addition, the apparent concentration of hydrogen in the 20 nm sample is found to be approximately 60× greater than that of the single crystal structure with regard to the permeation transients shown in Figure 2. The increased hydrogen diffusivity and capacity are attributed to high inter-crystalline content, which provides 1) a high density of short circuit diffusion paths and 2) large free volumes to which segregation of hydrogen can occur. Since the important parameter for "hydrogen release" is Permeability, which can be defined as the Diffusivity multiplied by the Solubility, the combined Permeability increase is 100×60, which equals a 6000-fold improvement in "hydrogen release" via nanostructuring. It is expected that this increased permeation will minimize embrittlement effects and play an important role in post-plating hydrogen bake-out heat treatments of high strength steels prone to HE. In addition, the electrodeposition of nanostructured materials tends to occur at very high current efficiencies (>90%), which already minimizes hydrogen uptake.
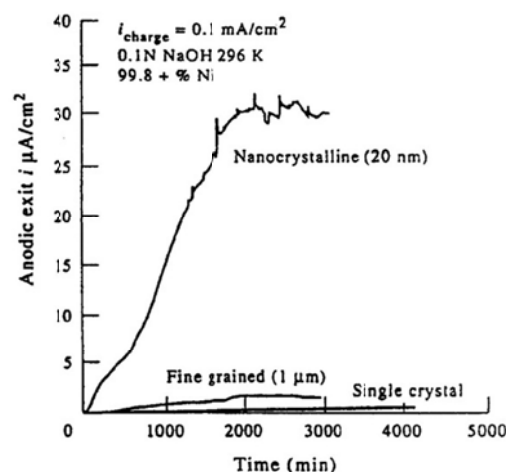
Figure 2: Hydrogen permeation transients showing anodic exit current density (flux) vs. time for nanocrystalline (20 nm), fine-grained (1 μm), and single crystal Ni foils [21,22].

As the process of producing nanostructured materials by electrodeposition relies on the use of applying pulse waveforms, it may be possible to further minimize hydrogen uptake through appropriate modification of the applied current waveforms. Specifically, recent electrodeposition research has shown that PR plating, as opposed to DC, can be used to achieve extremely broad concentrations of light gas impurities in the coating. For example, by simply modifying the PR waveform, the oxygen content of plated Ni was varied between 956 and 6039 ppm [23]. Hence, PR plating represents a promising tool with which the hydrogen uptake of the plating process can potentially be minimized. Since monatomic hydrogen is the species that diffuses into the high strength steel and ultimately causes embrittlement, the strategy here would be to determine which pulse waveform(s) promotes the re-combination of monatomic hydrogen (i.e. release from the surface) before it can diffuse and become entrapped within the steel microstructure. **The creation of a fully dense coating that is highly permeable to hydrogen via nanostructuring and the overall minimization of hydrogen uptake through the optimization of PP parameters are the central tenets of this initiative.**

As it pertains specifically to in service or hydrogen re-embrittlement (HRE) of the coated high strength steel substrate, it is anticipated that nanostructured coatings would be less susceptible to this phenomenon as compared to the porous Zn-Ni coatings that were developed in other development efforts since the "hydrogen release" of the nanocrystalline coatings is accomplished primarily via an intercrystalline diffusion mechanism as opposed to one that relies on bulk coating material porosity.

1.4   ENVIRONMENTAL IMPACT OF ZN-BASED COATINGS

With regard to potential environmental impact, it is anticipated that waste stream volumes will be, for all intents and purposes, identical to those currently experienced with Cd plating processes on a per tonne metal plated basis. However, the environmental impact of the wastes associated with the nanoscale deposition will be significantly reduced. Of the anticipated chemical constituents required for nanoscale Zn-based alloy deposition, some (e.g. Ni) are presently on the EPA lists of hazardous materials, although their impacts are considered more acceptable.

2.0   WORK OUTLINE FOR PROJECT PHASES

The objective of this program is to develop and optimize an advanced nanoscale Zn-based coating based upon modification of environmentally-benign commercial electroplating (wet) techniques which will

4

yield a coating process that meets or exceeds the overall performance (corrosion protection, torque-tension, etc.) and life-cycle cost of existing Cd electroplating and is particularly applicable to the coating of high strength steel fasteners. In order to achieve this objective, the coating process and structure must be engineered in such a way that any and all evolved hydrogen is minimized and/or prevented from diffusing into the steel substrate, not only during the coating process itself but also in-service (i.e. prevention of post-plate HRE).

The overall objectives for this project are to:

- Investigate the benefit of a nanostructured microstructure on the properties and performance of various commercial Zn-based alloy coatings, and
- Work on simple modifications to commercial electroplating techniques to develop an alloy that:
  - Meets or exceeds the overall performance (corrosion protection, torque-tension, HE, etc.) and life-cycle cost of existing Cd electroplating,
  - Provides a "Drop-in" replacement for Cd plating, capable of using existing Cd plating infrastructure.

This project will develop an understanding of the effect that microstructure (grain size, crystal structure (phase) and composition) has on the properties and performance (sacrificial corrosion, lubricity, HE) of Zn-based alloy coatings on high strength steel as a method to determine an optimal <u>microstructurally designed Cd-replacement coating.</u>

2.1   PHASE I WORK
The following task plan was followed during Phase I of this project.

TASK 1 – Identification of Nanoscale Commercial Coating Alloys
- Selected Zn-based binary alloys for investigation

TASK 2 – Laboratory Optimization of Nanoscale Zn-Based Alloys
- Lab scale experiments to optimize coating microstructure for each alloy system
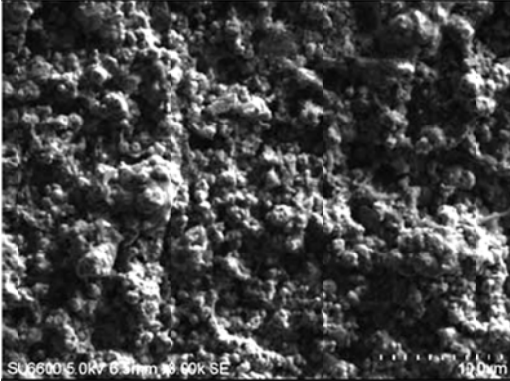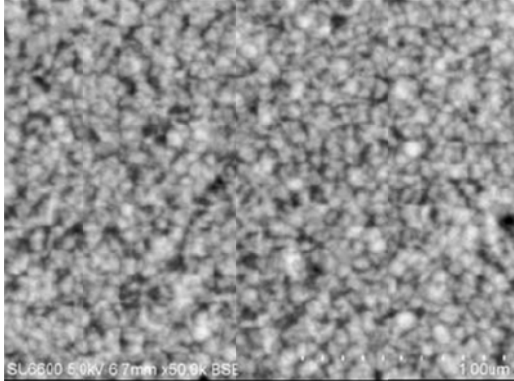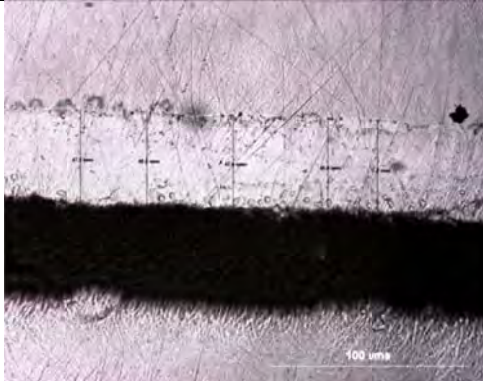
TASK 3 – Preliminary Characterization and Testing
- Screening testing to help development efforts in Task 2

TASK 4 – Coating Performance Evaluation on High Strength Steel
- Comparison of testing results of alloys with optimized microstructure

Four different commercial Zn-based alloys were investigated in Phase I: ZnNi, ZnCo, ZnNiCo and ZnFe. The ZnNiCo acid system was created by Integran, based on a commercial ZnNi acid chemistry. Viable Zn-alloy plating chemistries pursued for development as Cd-replacement coatings were compared from technical literature (academic and commercial) using a number of criteria. Hull cell investigations and 2 L beaker plating tests on mild steel substrates were performed to determine plating efficiency and rate. Coating appearance and surface morphology were investigated to confirm coating density (i.e. absence of macro-pores) and thickness uniformity, as well as effects of pulse plating and pulse-reverse plating. Examples are shown in Figure 3 for coatings produced in alkaline ZnNi baths. It is shown that pulse plating is shown to produce a deposit with: increased brightness, uniformity, and density; greater hardness and wear properties; grain refinement; and a more ideal single γ-phase microstructure for corrosion resistance. Further details regarding the system down-selection are provided in Appendix A.

a) Non-uniform DC Zn-Ni deposit with edge effects	b) Uniform PP Zn-Ni deposit with minimal/no edge effects
c) DC Zn-Ni deposit with rough, porous structure and 1-2 μm feature size	d) PP Zn-Ni deposit with smooth, dense structure and 70-100 nm feature size
e) Cross-section of Zn-Ni DC alkaline electrodeposit showing a rough, porous coating structure.	f) Cross-section of Zn-Ni PP alkaline electrodeposit showing a smooth, dense coating structure.

| g, cont.) XRD of DC deposit showing mixed-phase structure. | h, cont.) XRD of PP deposit showing single γ-phase structure and peak broadening. |
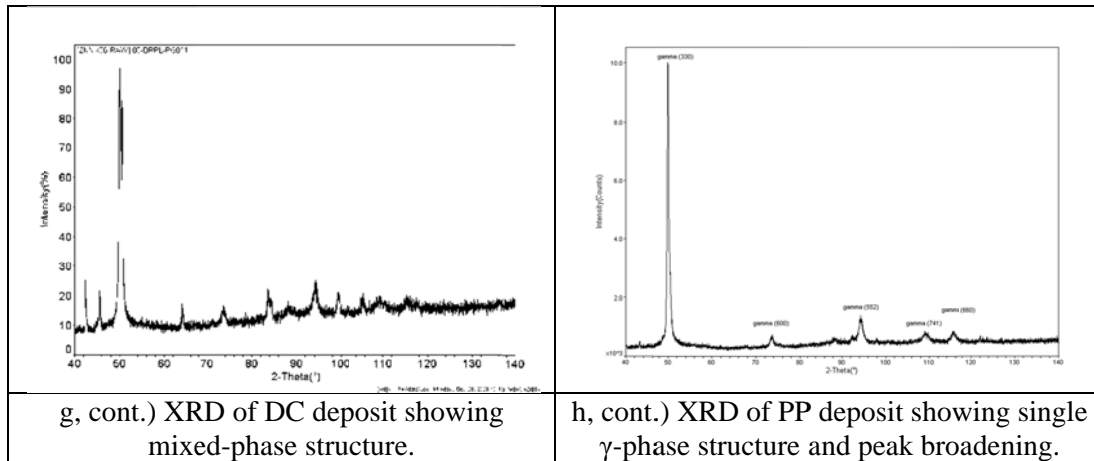
Figure 3: Macroscopic analysis, SEM micrographs, and XRD spectra of commercial zinc-nickel electrodeposits comparing direct-current (DC) (a, c, e, and g) and pulse-plated (PP) (b, d, f, and h) waveforms.

Furthermore, microstructure analysis was performed on the coatings to acquire their composition, microhardness, and grain size. Mechanical properties important for fastener applications, i.e. ductility and sliding wear, were also attained using standard test methods. Finally, characteristics of the deposit were analyzed such as adhesion, salt-spray corrosion (without chromate or chromium conversion coatings), torque-tension / lubricity friction, as well as preliminary hydrogen embrittlement (HE) testing (again without chromate or chromium conversion coatings). The Phase I results are summarized in Table 1.

Table 1: Summary of select Phase I results for this program.

Alloy	Electrical Waveform	Grain Size[3] (nm)	Hardness (VHN)	Salt Spray Corrosion (ASTM B117)[1]	Hydrogen Embrittlement (ASTM F519)	Torque-Tension (§3.4.2 of HSS JTP, 07/31/2003)[2]
Cadmium	DC	>100 nm	60	>1011	PASS	0.12
Zn-Ni Acid	DC	63	200	310 hours	PASS	0.21
	PP	32.7	290	699 hours	PASS	0.22
	PR	44.7	310	604 hours	PASS	0.17
Zn-Ni Alkaline	DC	51.6	270	705 hours	PASS	0.17
	PP	27.4	300	916 hours	PASS	0.15
Zn-Co Acid	DC	56.2	119	361 hours	PASS	0.20
	PP	58	96	427 hours	PASS	0.22
Zn-Fe Alkaline	DC	48	183	N/A	FAIL	0.14
	PP	39.5	231	N/A	PASS	0.17
Zn-Ni-Co Acid	DC	23.2	263	N/A	PASS	0.21
	PP	31.8	316	>1011 hours	PASS	0.19
	PR	21.4	131	>1011 hours	FAIL	0.17

Notes: [1]-Denotes hours to red rusting; [2]-Denotes torque friction (coefficients); [3]-Grain size determined by XRD

All process and property data were given a relative importance, and all the coatings were subject to a comprehensive evaluation matrix. Such metrics included: Plating rate; Current efficiency; Thickness uniformity; Bath stability; Grain size; Hardness; Ductility; Torque/Tension friction; Pin-on-disc friction; Salt-spray corrosion performance; and Hydrogen embrittlement performance.

A scoring matrix was developed to down-select specific alloy systems and plating chemistries for Phase II. A summary of the Phase I work and the Phase I scoring matrix are provided in Appendix A, Section 9.2, respectively. The most promising waveforms/Zn-Ni chemistries for Cd-replacement alternatives identified/down-selected were:

1. Pulse-plated Zn-Ni alkaline (based on the Atotech Reflectalloy ZNA system)
2. Pulse-plated Zn-Ni acid (based on the Enthone Zincrolyte CLZ-Ni 6340 system)
3. Pulse-plated Zn-Ni-Co acid (based on the Enthone Zincrolyte CLZ-Ni 6340 system)

These three systems were therefore carried forth for further development in Phase II. A Zn-Ni alkaline system is already being pursued by the Boeing Company as a Cd-replacement alternative on low strength steels. The Zn-Ni acid bath chemistry also showed a high degree of potential as a Cd-replacement coating, especially with regards to the uniform, dense coating produced by pulse-plated waveforms. And finally, the Zn-Ni-Co ternary alloy showed the most interesting combination of physical properties when plated with pulse-plating conditions. As well, it is a novel bath chemistry based on the commercial Zn-Ni acid system, and therefore may be the most promising of the three Cd-replacement systems chosen for further development in Phase II.

2.2 PHASE II WORK

Phase II activities concentrated on scaling up the selected systems for bulk coating of high strength steel fasteners, namely the Zn-Ni alkaline, Zn-Ni acid, and Zn-Ni-Co acid plating chemistries. Further investigation of these Zn-based alloy systems were performed to ensure that the coating properties are maintained with a 40 L scaled up system. As well, optimization activities were performed to investigate the possibility of further improving coating properties. Optimization included use of known techniques as well as techniques proprietary to Integran and developed in other programs. Long-term bath use was studied to demonstrate reproducibility and process consistency. It is imperative that the selected baths and conditions are repeatable in plating and performance in any volume of bath for any method of plating. Since the end application is high strength steel fasteners, the scaled up bath will also be tested using a barrel-plating mechanism which is typical of fastener plating; tests in Phase I focused on rack-plating.

A critical component of Phase II surrounded the performance of down-selected Zn-based alloy coatings in hydrogen re-embrittlement (HRE) testing. As HRE is a critical requirement of the in-service performance of sacrificial coatings on high strength steel, HRE testing was focused on during Phase II activities. Although coating porosity supposedly minimizes HRE, it is expected that the fully-dense, ductile, nanocrystalline coatings produced by pulse plating will perform well in HRE testing due to other physical properties.

The following workplan was followed for Phase II of this project:

TASK 5 – Optimization of Specific Nanoscale Alloys
- Further optimize down-selected nano-scale alloy chemistries to develop a consistently ultra-high efficiency process that produces deposits with target microstructure and properties

TASK 6 – Evaluation of Cr^{6+}-free Conversion Coatings
- Post-plate Cr^{6+}-free conversion coatings (e.g. environmentally benign trivalent chromium, Cr^{3+}) will be investigated to be paired with the Cd-replacement coating that emerges from this program

TASK 7 – Sample Production and Testing
- Perform a thorough testing regimen on the optimized Cd-replacement + conversion coating structure

8

- o Hydrogen Embrittlement (HE) – ASTM F519
- o Salt spray corrosion – ASTM B117
- o Taber wear / pin-on-disc friction
- o Torque-tension
- o Hydrogen re-embrittlement (HRE) – after ASTM F519

TASK 8 – Comprehensive Coating Performance Evaluation
- Evaluate for high-strength steels the general performance of selected nanoscale Zn-based coating systems relative to current Cd-plating processes

TASK 9 – Rack/Tank/Barrel Plating Evaluation
- Investigate the compatibility of the selected processes with conventional production plating techniques, such as high volume barrel plating

3.0   TASK 5 – OPTIMIZATION OF SPECIFIC NANOSCALE ALLOYS

3.1   TASK OBJECTIVES
The objectives of Tasks 5, 6, and 7 were to further optimize the alloys selected in Phase I (namely, commercial alkaline Zn-Ni and acid Zn-Ni, and modified acid Zn-Ni-Co) with emphasis placed on the development of a **consistently** ultra-high efficiency process **in a scaled-up bath** that produces 1) deposits with microstructures facilitating rapid hydrogen diffusion out through the coating, and 2) deposits with microstructures providing enhanced protection from corrosive environments which are conducive to premature part failure (i.e. in-service embrittlement).

3.2   SCALE-UP OF BATHS TO 40 L VOLUMES
In order to further refine the choice of bath for large-volume plating, the three baths selected in Phase I were scaled up from 2 L volumes to 40 L volumes.

3.2.1   Zn-Ni alkaline
The Zn-Ni alkaline bath chemistry developed in Phase I (based on the Atotech Reflectalloy ZNA system) was scaled up to 40 L, shown in Figure 4. Design of Experiments (DoEs) were conducted to evaluate the 40 L-plating functionality, including: running Amp-hours through the bath and monitoring bath stability, bath composition, cathodic efficiency, deposit quality, composition and microstructure. Example results are presented in Section 3.2.3. In addition, additive studies were conducted to determine an appropriate replenishment schedule for metals as well as chemical additives. Custom racks were designed and built in order to enable simultaneous plating of: 1) multiple flat samples of mild steel (MS) for composition, thickness, grain size, and ductility testing, as well as Taber wear measuring; 2) multiple plates of high-strength steel (HSS) for ASTM B117 corrosion testing; 3) multiple HSS notched bars for ASTM F519 HE and HRE testing; and 4) multiple HSS bolts for torque-tension testing.

Phase II of this work also investigated an alternative Zn-Ni alkaline commercial system: Zn-Ni PLUS system, Dipsol IZ-C17+, Low Hydrogen Embrittlement Alkaline. This system has been considered a benchmark for minimal hydrogen embrittlement and re-embrittlement protection. According to the Technical Data Sheet provided by Dipsol of America, the bath produces deposits consisting of 12-18 wt.% Ni, hardness of 350-450 kg/mm^2 VHN, and plating rates between 0.35 – 0.45 μm/min. at a typical current density of 50 mA/cm^2. In the present Phase, the Dipsol system was compared to that of Atotech, providing comparative data for hydrogen re-embrittlement and salt-spray corrosion testing.

Figure 4: Image of 40 L (10.5 gallon) Zn-Ni alkaline plating set-up.

Optimization included determining the optimal current density for the use of known pulse plated waveform techniques (e.g. PP) as well as novel pulse-reverse (PR) waveform parameters proprietary to Integran that were developed in other programs. The test results demonstrated that the target fully-dense and uniform coatings can be produced using both pulse-plating (PP) and pulse-reverse plating (PR) electrical waveforms. Inter-run data outlined good bath stability data and a consistent replenishment schedule which could be followed to produce repeatable coatings. It was found that the deposit composition and efficiency were the primary variables that could be adjusted and/or tailored with the electrical waveform. For example, Figure 5 illustrates that the composition and efficiency are closely related:
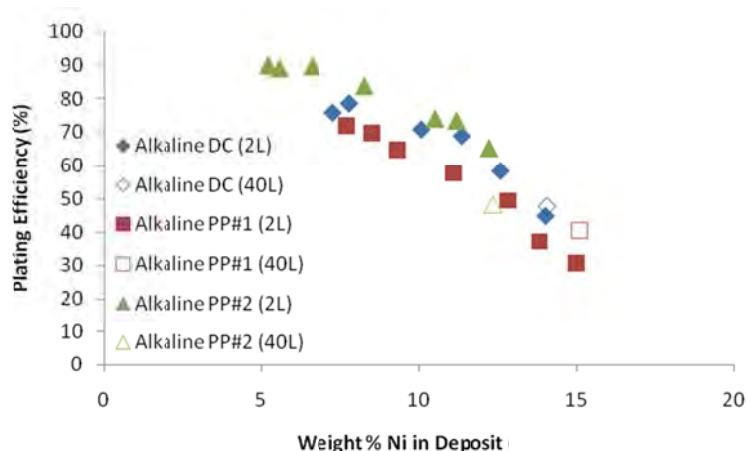
Figure 5: Relationship between composition and plating efficiency in the Zn-Ni alkaline system. Two separate PP conditions are shown, which utilize duty cycle/frequency of 10%/90Hz and 50%/10Hz, respectively.

These results were used to establish optimal process windows for DC and PP deposition. In particular, the optimal composition was targeted, which influences the open-circuit potential of the coating as well as the corrosion uniformity. For example, it is well-known that the single γ-phase in Zn-Ni alloys (between

approximately 13 and 24 wt.% Ni) is desirable for strength, ductility, and corrosion requirements. The results found in this Task show that this composition range can be approached in the present alkaline system with a reasonable plating efficiency.

In addition to MS substrates, HSS samples have also been successfully plated using these optimal process windows. In this case, however, suitable activation processes were required to develop good adhesion between the coating and the substrate. Figure 6 displays an example HSS plaque DC-plated using the 40 L alkaline Zn-Ni system. In this case, the composition was measured as 8 wt.% Ni, and the thickness as 17 microns. The chromium conversion coating (trivalent, Atotech) can be easily observed, indicating an acceptable coating for conversion.
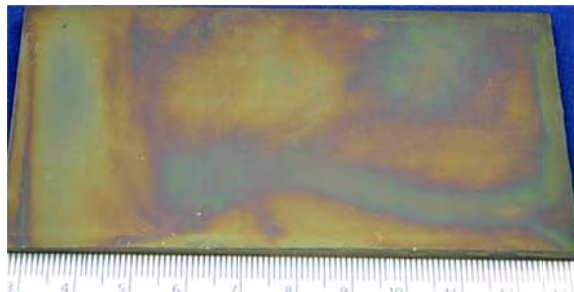
Figure 6: Example HSS plaque DC-plated with Cr^{3+} conversion coat for ASTM B117 corrosion testing.

Plating rates were measured throughout an example period of bath use. In the case of DC plating as defined for the proprietary bath chemistry, the plating rate was measured between 0.25 – 0.40 µm/min. PP waveforms yielded similar plating rates that depended largely upon the waveform used (Figure 7):
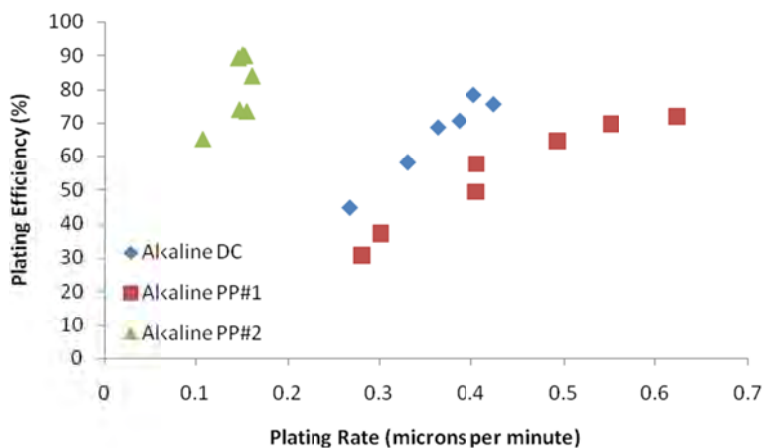
Figure 7: Relationship between plating conditions, rates, and efficiencies for the Zn-Ni alkaline system. PP#1 and PP#2 utilize different duty cycles (same as Figure 5).

3.2.2 Zn-Ni acid

The Zn-Ni acid bath chemistry developed in Phase I (based on the Enthone Zincrolyte CLZ-Ni 6340 system) was scaled up to 40 L, shown in Figure 8. Similar to the alkaline bath, a DoE was performed in order to evaluate the 40 L-plating functionality, including: running Amp-hours through the bath and monitoring bath stability, bath composition, cathodic efficiency, deposit quality, composition and microstructure. Example results are presented in Section 3.2.3. It was determined that the acid bath had somewhat less stability than the alkaline bath, primarily due to 1) the consumable anodes used in the

former and the observed passivation of Zinc chips which would have to be re-activated, and 2) the replenishment of buffer NH_4Cl which is required in large amounts. However, like the alkaline bath, a replenishment schedule was outlined for consistent and repeatable deposits. Optimization included use of known waveform techniques (e.g. PP) as well as techniques proprietary to Integran and developed in other programs (PR). Optimal process windows for DC, PP, and pulse-reverse plating (PR) were established, producing zinc alloys with nickel contents desirable for strength, ductility, and corrosion requirements. Similar to that for alkaline Zn-Ni plating, a close relationship was observed between plating efficiency and composition (Figure 9). The use of PR waveforms was found to allow for much higher Ni contents, but this is achieved only with a very low efficiency. In these cases, plating rates can vary between approximately 0.8 microns per minute for the highly-efficient low-Ni deposits to 0.01 micron per minute for high-Ni deposits.

Figure 8: Image of 40 L (10.5 gallon) Zn-Ni acid plating chemistry.
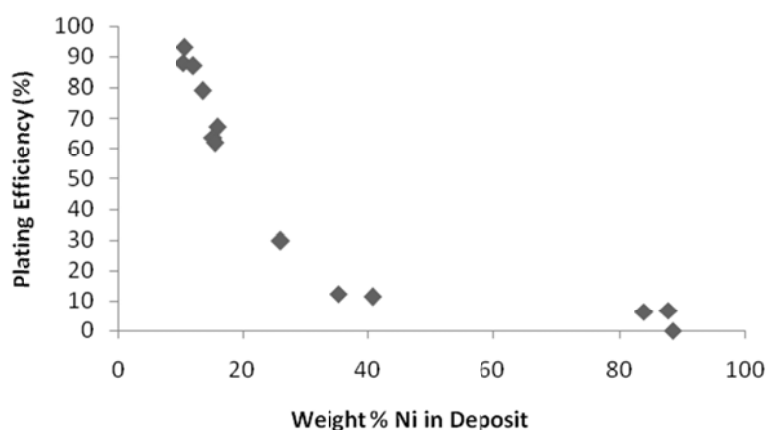
Figure 9: Relationship between composition and plating efficiency for samples produced using pulse reverse conditions in the Zn-Ni acid system.

3.2.3 Optimization of Nanoscale Alloy Production with Binary Zn-Ni Systems
As outlined in Sections 3.2.1 and 3.2.2, a number of DoEs were performed to determine the stability of the scaled-up baths as well as determine the optimal nanoscale alloy production. Particularly, bath stability (i.e. chemical constituent levels) was monitored as a function of usage (i.e. Amp-hours/liter) to

determine 1) window of operation limits, 2) organic decay and treatment procedures, and 3) a chemical replenishment schedule. For example, Figure 10 presents the metal constituent levels as a function of DC bath usage in the Zn-Ni alkaline system, and Figure 11 presents the deposit composition as a function of the same.
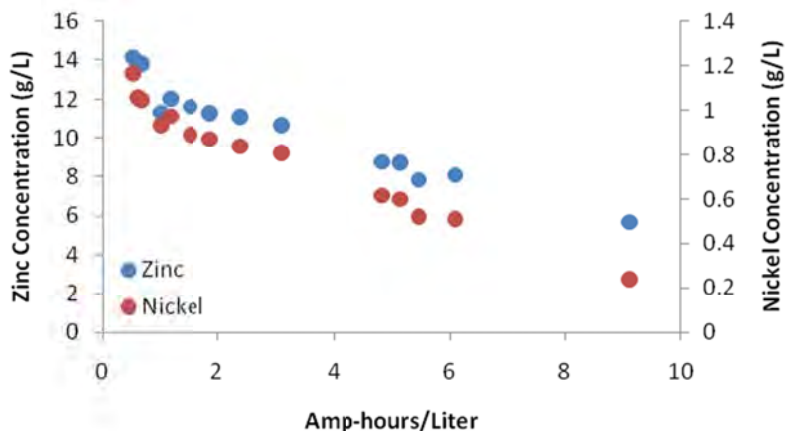
Figure 10: Metal constituent levels as a function of DC bath usage in the Zn-Ni alkaline system.
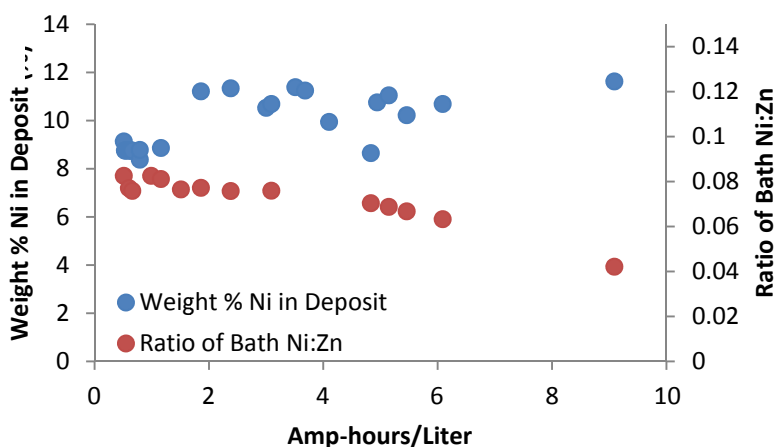
Figure 11: Deposit composition as a function of DC bath usage and metal levels in the Zn-Ni alkaline system.

3.2.4 Improvements of Pulse Plating over Direct Current Plating with Binary Zn-Ni Systems

As shown in the Phase I work, there is a significant advantage to using pulse plating approaches over DC approaches in commercial binary Zn-Ni chemistries. For example, it was shown that the use of brighteners in the Zn-Ni acid DC system promoted a single-phase γ microstructure. When the brighteners were removed, a mixed-phase microstructure resulted from DC plating, which is less desirable from a corrosion standpoint. In contrast, plating under a pulsing waveform and without brighteners could restore the single γ-phase and reach a fully-dense microstructure.

Additional comparisons between DC plating and pulsing approaches were also investigated in Phase II, namely the uniformity of deposit thickness on an angled substrate. Figure 12 shows an angled steel 4"×4" cathode, bent 60°, and with the apex placed 6" from the anode in the Zn-Ni acid bath. The composition and thickness was measured at points along the cathode (Figure 12) for both DC and PR conditions (Figure 13).

Figure 12: Angled cathode used to investigate plating uniformity between DC and pulsing approaches.
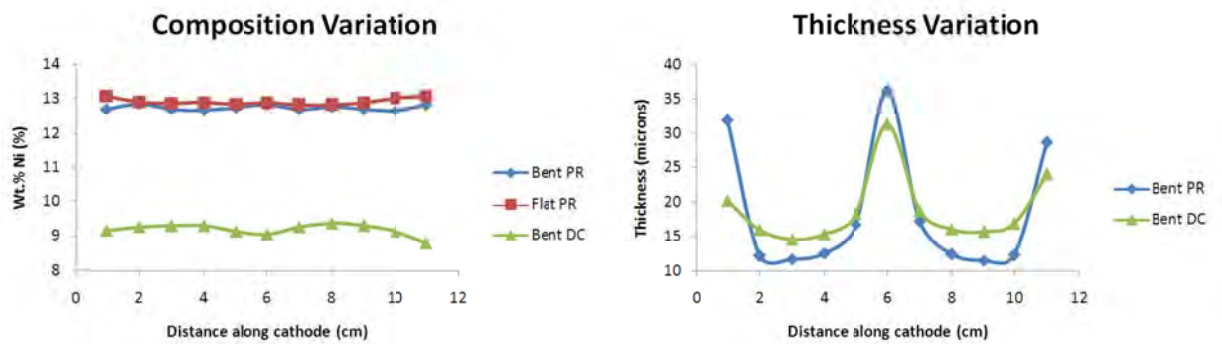
Figure 13: Differences in composition (left) and thickness (right) uniformity on an angled cathode using DC and PR approaches in Zn-Ni acid. The mark of 6 cm denotes the apex of the cathode.

In Figure 13, it can be seen that while the thickness variation is greater on the PR cathode, its composition is more uniform than the DC deposit. This is a critical component for corrosion protection, as the response (i.e. open circuit potential and corrosion current) are highly dependent on the alloy composition. This, combined with the composition approaching the desired Ni levels for a single γ phase, suggests superior corrosion uniformity using pulse plating techniques. In addition, it was found that pulse-reverse plating led to an increased wt.% Ni content in the same bath. Similar results were observed for the alkaline system (Figure 14). In this bath, however, the throwing power was improved over the acid bath, as observed by the more narrow range of thickness.
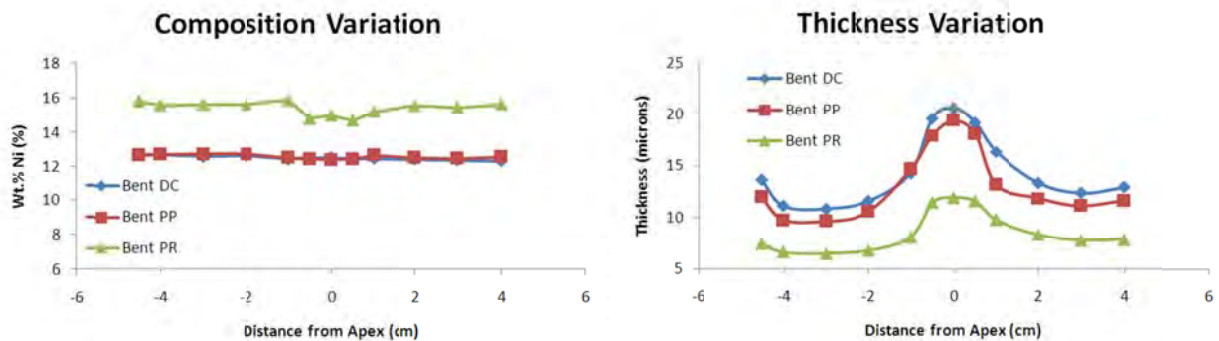
Figure 14: Differences in composition (left) and thickness (right) uniformity on an angled cathode using DC, PP, and PR approaches in Zn-Ni alkaline (Dipsol). The mark of 0 cm denotes the apex of the cathode.

3.2.5 Zn-Ni-Co acid

A number of DoEs were performed with the Zn-Ni-Co acid system in an effort to investigate the effect of plating parameters on coating composition and ductility, and ultimately to find an optimal processing window and replenishment schedule to scale up to a 40 L volume. Optimization included use of known waveform techniques (e.g. PP) as well as techniques proprietary to Integran and developed in other programs (PR). DoE variables included pH, temperature, plating conditions (DC, PP, and PR) as well as current densities. Deposits possessed promising ductilities, and lower wt.% Zn deposits could be achieved (i.e. into the desirable γ-phase), overall making this system attractive. Promising plating conditions have been found for all three plating conditions, i.e. DC, PP, and PR, which largely mirror those for the Zn-Ni acid bath. However, it was found that the replenishment schedule for this bath was more complex than the binary Zn-Ni systems. This bath was therefore not scaled up to a 40 L volume. Nonetheless, the 2 L volume was used to produce samples for Task 6 and compare with the two binary Zn-Ni deposits.

4.0 TASK 6 – EVALUATION OF CR^{6+}-FREE CONVERSION COATINGS

4.1 TASK OBJECTIVES

In this Task (as outlined in Section 3.1), the effectiveness of chromate and chromium conversion coatings on the deposits produced was investigated using the three down-selected Zn-based alloy coatings. ("Converting" will henceforth refer to the application of chromate or chromium conversion coatings.)

The acceptance of the chromate and chromium conversion coatings (or "conversion", for short) was primarily evaluated optically, where typical color changes could be used to denote proper coating. Chromate and chromium conversion coatings were applied primarily to 1) plated mild steel (MS) test pieces, and 2) plated HSS plaques designated for salt-spray corrosion testing (ASTM B117). Three conversion coatings were investigated for the Zn-alloy plated HSS pieces: Enthox (30% 7701M, hexavalent chromium), Atotech EcoTri (5% Reagent B, trivalent chromium), and for the Dipsol LHE Zn-Ni system, the trivalent chromium conversion coating system IZ-264 was used. For each plating bath (Zn-Ni acid, Zn-Ni alkaline, and Zn-Ni-Co acid) a suitable conversion coating was determined. In addition, the influence of sample surface was investigated, including time between plating completion and bake-out and effect of post-bake re-activation. Further evaluation of conversion coating effectiveness was performed following salt-spray corrosion testing.

4.2 QUALITATIVE ANALYSIS OF CONVERSION COATINGS

In the case of the hexavalent chrome product (Enthox), yellow coloration is typically observed. In contrast, the trivalent chromium product (Atotech) typically displays a blue or clear coloration.

4.2.1 DoE for Converting Time and Solution Concentration

A Design of Experiments (DoE) was carried out on plated MS pieces using the Zn-Ni alkaline system. The recommended operating procedures for the respective conversion treatments included in the respective Technical Data Sheets (TDS) was appropriate for all waveforms, e.g. (Figure 15a and b). It was also noted, that longer conversion times were required for the trivalent system as its usage increased, e.g. from a range of 30-90 seconds (Figure 15a) to between 1.5 and 9 minutes (Figure 15c). It is clear that in these samples, there is a significant color variation across the test samples. According to the TDS for the IZ-264 trivalent chromium conversion coating, color variation may be due to a number of factors, including insufficient rinsing, temperature variation in rinsing, conversion thickness variations, localized Zn-Ni deposit thickness and/or composition, or even localized substrate variations. It is not known how closely linked color variation is to localized corrosion protection; this will be investigated in the following sections.
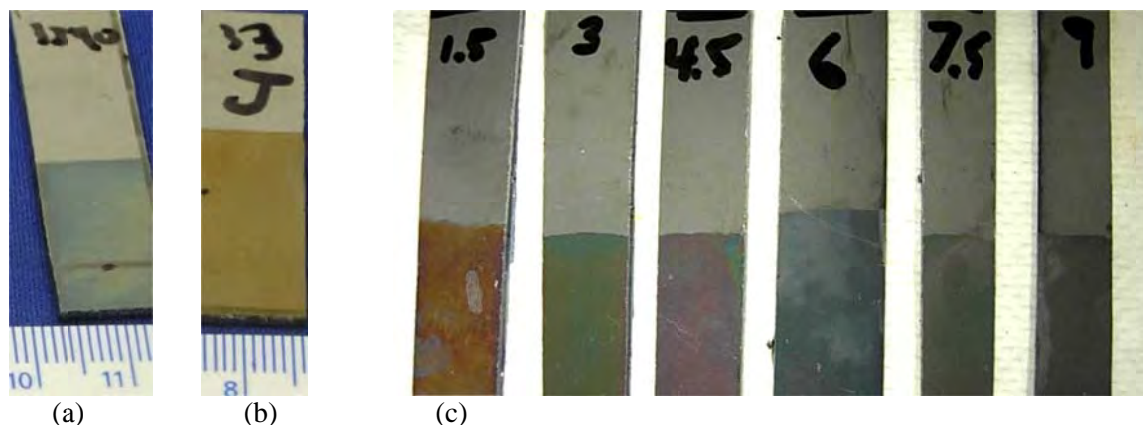
Figure 15: Conversion coating DoE on Zn-Ni alkaline plates. (a) typical Cr^{3+} conversion with clear/blue coloration (90 second immersion), (b) typical Cr^{6+} conversion with yellow coloration, and (c) effect of trivalent conversion time as the bath life increased (numbers denote minutes from 1.5 to 9).

4.2.2   Zn-Ni alkaline HSS Plaques

Figure 16 presents plated HSS plaques converted with the two products. All bars appear to have been converted successfully, independent of the deposit composition (between 8-10 wt.% Ni) and waveform (DC and PP). Again, there is a color gradient within the conversion coat, mostly in the Cr^{3+} system.
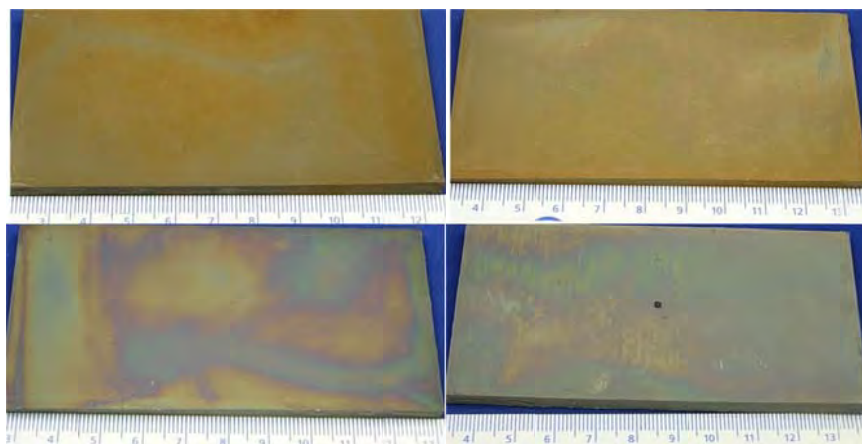
Figure 16: Zn-Ni alkaline DC (left) and PP (right) HSS converted – Enthone (top) and Atotech (bottom).

4.2.3   Zn-Ni acid HSS Plaques

Figure 17 presents plated HSS plaques converted with the two products. Similar to the alkaline case, all bars appear to have converted successfully, independent of the composition (8-12 wt.% Ni) and waveform (PP and PR). It is worth noting that the Enthone coating was not prominent on the PR sample, which had 12 wt.% Ni. The color gradient is most pronounced on the hexavalent chromium conversion coating, while the trivalent chromium conversion coating color appears more uniform.

16
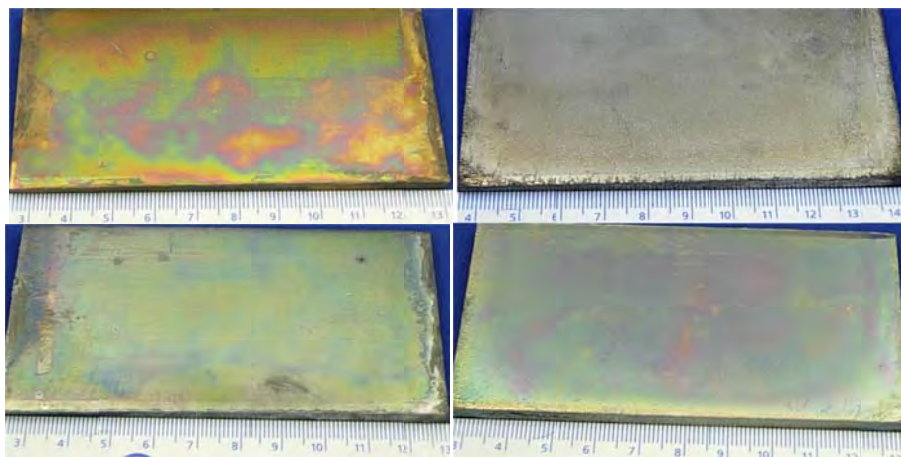
Figure 17: Zn-Ni acid PP (left) and PR (right) HSS converted – Enthone (top) and Atotech (bottom).

4.2.4   Zn-Ni-Co acid HSS Plaques

Figure 18 presents plated and converted Zn-Ni-Co HSS plaques. Similar to the previous cases, all bars appear to have converted successfully, independent of the composition (11-15 wt.% Ni+Co) and waveform (PP and PR). It is worth noting that the Enthone conversion coating did not possess the same coloration as the PP sample, which had 11 wt.% Ni+Co.

Figure 18: Zn-Ni-Co acid PP (left) and PR (right) HSS converted – Enthox (top) and Atotech (bottom).

Based on the observed plated pieces, it appears that the trivalent chromium conversion coating (Atotech) is easier to detect, and that it is detectable on all of the plated HSS parts over a range of compositions. Salt-spray corrosion test results (presented in Section 5.3) will be considered to compare the performance of the two coatings.

4.2.5   Novel Organic / Inorganic Hybrid Coating Substitute

In addition to the trivalent chromium conversion coating as a substitute for a hexavalent counterpart, Phase II also investigated a novel organic/inorganic hybrid coating based on polymeric cross-linking reactions and inorganic Sol-Gel chemistry. The coating was developed by Prof. Vreugdenhil at Trent University (Peterborough, Ontario), and has previously shown promise both as a corrosion inhibitor and lubricant.

17

While the conversion coating process produces a chemical bond to the Zn-Ni layer, it was determined that additional processing steps were needed to achieve good adhesion between the Zn-Ni layer and Sol-Gel layer. Namely, it was found that dilute HCl activation as well as citric acid activation treatments (both recommended in the Dipsol Cr^{3+} conversion coating TDS) were unsuccessful. More recently, cleaning the samples with a dilute phosphoric acid treatment was found to lead to good adhesion, but at the expense of a number of fine surface cracks and some deep cracks in the Zn-Ni coating (Figure 19). IR spectrum analysis of the cleaned samples suggested that a residual phosphate on the surface of the Zn-Ni coating was the primary cause of good adhesion; XRF analysis showed that the phosphoric acid treatment led to minimal thickness loss as well as a slight increase in wt.% Ni in the deposit (Figure 19). This was therefore considered a suitable surface treatment for initial trials with Sol-Gel coatings.
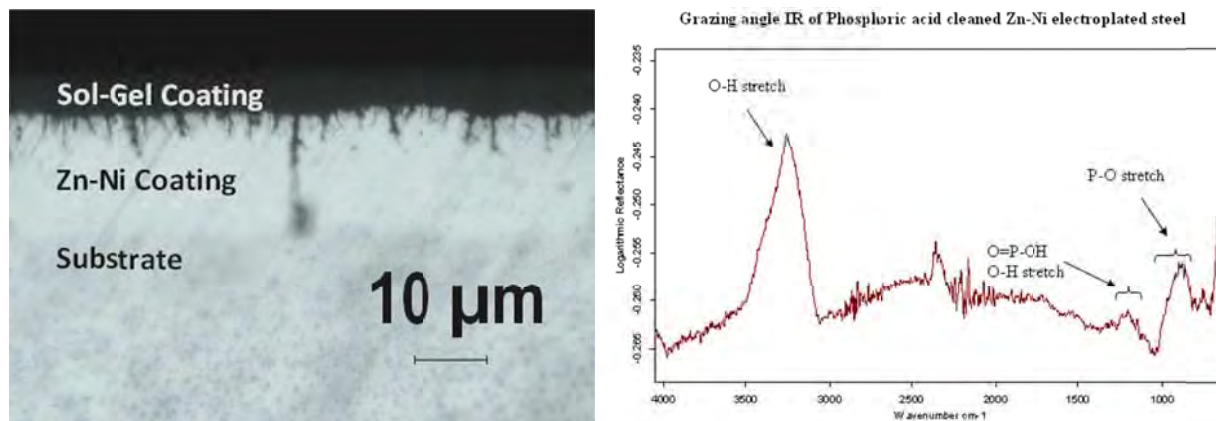
Figure 19: Cross-section of a Zn-Ni alkaline plate given phosphoric acid treatment and Sol-Gel coating. Also shown is the IR spectrum of the coating on Zn-Ni substrate, displaying phosphate remaining on the surface.

5.0   TASK 7 – SAMPLE PRODUCTION AND TESTING

5.1   TASK OBJECTIVES
The objective of Task 7, in addition to that outlined in Section 3.1, was to compare the performance of the three down-selected Zn-based alloy coatings with respect to environments where Cadmium coatings are used. This includes five primary tests:

1. Hydrogen Embrittlement (HE) – ASTM F519
2. Salt Spray Corrosion – ASTM B117
3. Taber Wear / Pin-on-Disc Friction
4. Torque-Tension
5. Hydrogen Re-Embrittlement (HRE) – after ASTM F519

5.2   HYDROGEN EMBRITTLEMENT (HE) TESTING – ASTM F519
For this test, 4340 HSS ASTM F519 type 1a1 notched tensile bar were plated and sent to Omega Research Inc. (Justin, TX) for testing. All plated notched tensile bars were given a bake-out treatment before testing using the standard condition (191°C for 24 h). Four test samples were required for each plating condition, after ASTM F519. Each sample was loaded to a value of 75% the Notch Fracture Strength (NFS) and sustained up to 200 hours; failure to hold for 200 hours was considered a failure. Plating in all cases was done to a thickness according to the AMS 2417G standard, i.e. between 8-18 microns on un-notched surfaces "with visual evidence of plating at the root of the notch." All samples were left in the un-converted condition and were activated prior to plating by an acidic HE bar surface activation procedure. Figure 20 presents an example of a plated HE test sample produced using the Zn-Ni

acid bath. The coating in this case is fully-dense and covers the entire notch: the thickness is ~37 microns outside the notch, and ~18 microns within it. Table 2 summarizes the results for the three down-selected systems produced and their respective waveforms; also included are the results for the Cd benchmarks. Phase II.2 consisted of samples plated only using the Dipsol alkaline system, whereas in Phase II.1 the Atotech system was used for alkaline bath plating.
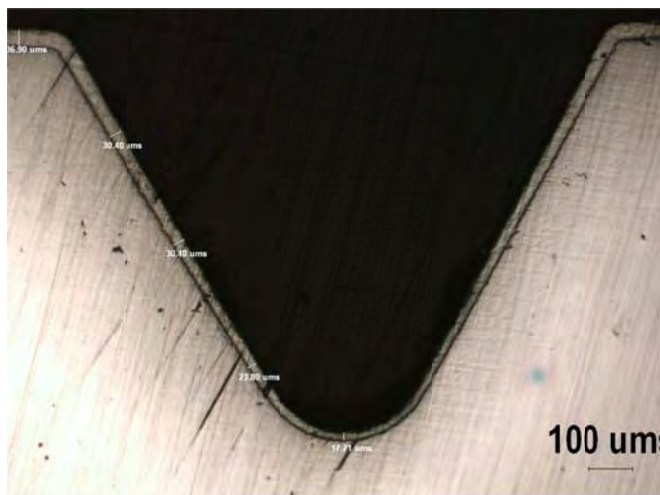
Figure 20: Example cross-section of an ASTM F519 type 1a**1** notched tensile bar plated with Zn-Ni acid.

Table 2: Summary of ASTM F519 HE results for down-selected Zn-based alloys.

Alloy	Electrical Waveform Optimized	Phase I Pass/Fail	Phase II.1 Pass/Fail	Phase II.2 Pass/Fail
Cadmium	DC	PASS		
Zn-Ni alkaline (Phase II.1: Atotech Phase II.2: Dipsol)	DC	PASS		PASS
	PP	PASS	PASS	PASS
	PR			PASS
Zn-Ni acid	DC	PASS		
	PP	PASS	PASS	
	PR	PASS	FAIL	
Zn-Ni-Co acid	DC	PASS		
	PP	PASS	PASS	
	PR	FAIL	FAIL	

In most cases, the results obtained in Phase II were similar to those from Phase I: the majority of the zinc-nickel coatings were observed to pass. However, while HE bars produced using PP approaches passed, those produced using PR waveforms tended to fail testing – except in the case of the Zn-Ni alkaline Phase II.2 (performed using the commercial Dipsol bath). In an acid bath, this failure may be due to the difference in composition: PP deposits typically possess lower wt.% Ni than PR deposits, leading to a lower plating efficiency (e.g. Figure 5 and Figure 9) and therefore more hydrogen inclusion in the steel substrate. In contrast, the alkaline baths already possess low efficiency that pulse-reverse plating does not greatly change the effect of hydrogen inclusion.

5.3   SALT SPRAY CORROSION – ASTM B117
For this test, 4340 HSS plaques were plated (e.g. Figure 16 – Figure 18) and sent to Acuren Group Inc. (Mississauga, Ontario) for salt-spray corrosion testing after ASTM B117. There were two iterations in this Phase: the first (II.1) compared un-scribed, converted samples to non-converted samples, and was

performed solely on HSS plaques; the second (II.2) focused on a single conversion treatment and included both HSS plaques as well as bolts in both the scribed and un-scribed conditions. Plating in all cases was done to a thickness between 10-18 microns. All samples were tested in a salt-spray chamber for a 1000-hour duration, over which the existence of white and red rust was monitored.

Table 3 summarizes the results for the Phase I three down-selected Zn-based alloy systems. The Phase II.1 converted samples used both the Cr^{6+} (Enthone) and Cr^{3+} (Atotech) coatings, which were applied according to AMS 2417G Type I. Examples of un-scribed plaques before and after testing are shown in Figure 21. The Cadmium benchmark plaque displayed no white or red rust after 1000 hours. In contrast, the Zn-Ni acid PR (12 wt.% Ni) plaque without conversion coating displayed significant white rust after 1000 hours. Furthermore, the Zn-Ni acid PR (12 wt.% Ni) plaque with Cr^{3+} conversion coating displayed no white or red rust after 1000 hours. The results from the ASTM B117 tests lead to a number of conclusions: that the Cr^{3+} chromium conversion coating performs similar to its Cr^{6+} counterpart; that the existence of a conversion coating vastly improves the corrosion response of the plaques; and that all but one Zn-Ni plaque resists the development of red rust by forming a sacrificial coating. However, the alkaline (Atotech) plaques all quickly developed white rust which may lead to undesirable mechanical properties, but none developed red rust. Finally, the existence of a scribe in the corrosion sample further demonstrates the efficacy of the Zn-Ni coatings, displaying their sacrificial properties to resist significant red rust formation (Figure 22). However, the extent of white rust formation varied between Phase II.1 and II.2 deposits. This was independent of scribing, which suggests that the coating retained its sacrificial composition but that other factors exist in overall corrosion resistance.

Table 3: Summary of ASTM B117 salt-spray corrosion results for down-selected Zn-based alloys. Numbers denote hours to white and red rusting.

Alloy	Electrical Waveform Optimized	Phase II.1 No Cr Un-Scribed White/Red	Phase II.1 Cr^{3+} Un-Scribed White/Red	Phase II.1 Cr^{6+} Un-Scribed White/Red	Phase II.2 Cr^{3+} Un-Scribed White/Red	Phase II.2 Cr^{3+} Scribed White/Red
Cadmium	DC	> 1000				
Zn-Ni alkaline (Atotech)	DC	< 150	< 150	< 150	< 150	< 150
	PP	< 150	< 150	< 150	< 150	< 150
Zn-Ni alkaline (Dipsol)	DC				~800	~800
	PP				~800	~800
	PR				~800	~800
Zn-Ni acid	DC				< 150	< 150
	PP	< 150	~ 700	~ 600	< 150	< 150
	PR	< 150	> 1000	~ 360		
Zn-Ni-Co acid	PP	< 150	~ 850	~ 360		
	PR	< 150; ~ 360	> 1000	> 1000		

(a, before and after)   (b, before and after)   (c, before and after)
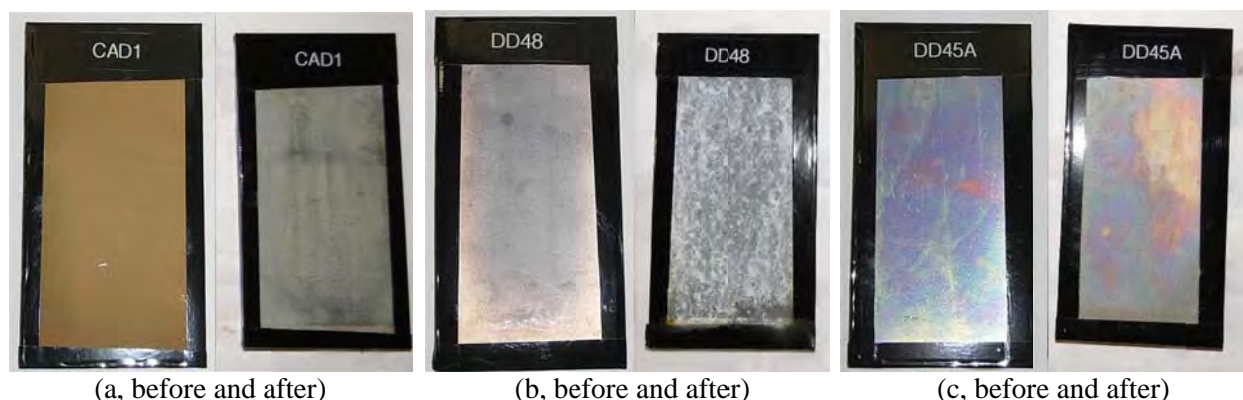
Figure 21: Example un-scribed plated HSS plaques before and after ASTM B117 testing: Cadmium (a), un-converted Zn-Ni acid PR (b), and Cr^{3+}-coated Zn-Ni acid PR.
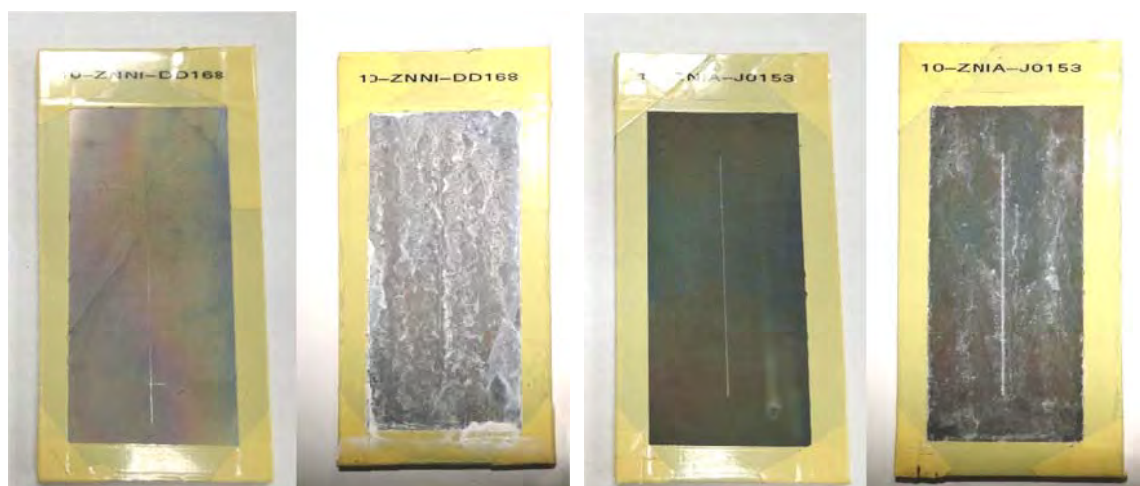
Figure 22: Example scribed plated HSS plaques before and after ASTM B117 testing: Zn-Ni acid PP (left) and Zn-Ni alkaline PP, Atotech (right). Acid PP deposit has full white rust formation after <150 h, independent of scribing, whereas the alkaline PP deposit shows reduced white rust coverage after 1000 h.

In particular, Phase II.1 acid-PP (Cr^{3+}) samples, which possessed composition of 8.4 wt.% Ni and were made using brand-new conversion solution, resisted white rust formation until ~600 h; in contrast, similar samples in Phase II.2 (10.9 wt.% Ni deposit composition, but after significant conversion solution usage) formed white rust in under 150 h. There are a number of factors which can influence the efficacy of the conversion coating; these include not only properties of the deposit (e.g. wt.%Ni) but also the conversion coating solution characteristics – such as level of Cr precipitation and impurity concentration in the trivalent chromium system. As a result, the uniformity of the conversion coating may depend on the state of the conversion solution (usage, impurity content, etc.), which may lead to different patterns in white rust formation.

The present results also suggest an influence of both coating composition and surface morphology on the corrosion response. For example, shown in Figure 23 is a Zn-Ni alkaline PP deposit (prior to conversion coating) with a composition of 9.2 wt.% Ni. Also shown in Figure 23 is a Zn-Ni acid PP deposit (prior to conversion coating) with a composition of 8.5 wt.% Ni. Despite the similarities in composition, the converted alkaline plaque developed white rust in under 150 hours, whereas the converted acid plaque did not develop white rust until after 600 hours.
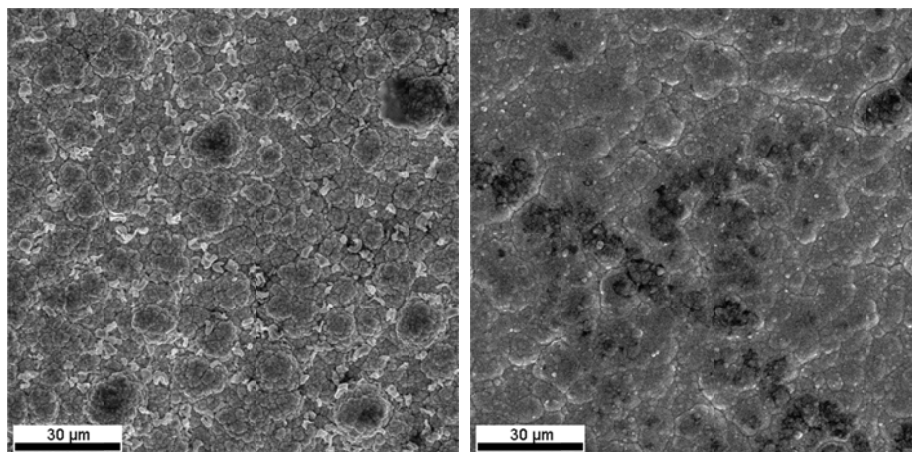
Figure 23: Example surface morphologies of (left) Zn-Ni alkaline PP (9.2 wt.% Ni) and (right) Zn-Ni acid PP (8.5 wt.% Ni) coated HSS plaques prior to chromating and corrosion testing.

The issue of rust uniformity and time to formation may also be related to the gradient of coloration found on the panels following conversion. Conclusions could not be drawn from these tests as there were inconsistent results between panels which overall had a wide range of deposit characteristics.

Plated fasteners were also tested during Phase II.2 in salt-spray corrosion (Figure 24) in the un-scribed condition or the scribed condition. Similar to the case for the plated steel plaques, faster red rust formation occurred on the acid Zn-Ni fasteners, independent of a pre-existing scribe. Only mild white rust was found in the Atotech alkaline Zn-Ni DC and PP fasteners after 1000 h. The difference between results from fasteners (Figure 24) and steel plaques (Table 3) may be due to the composition and thickness variation across the fastener threads: high current-density areas (thread peaks) will generally possess thicker deposits larger in wt.% Ni, whereas low current-density areas (thread valleys) will generally possess thinner deposits with lower wt.% Ni (e.g. see HE bar in Section 5.2). The larger fluctuation in polarization across the fastener may therefore lead to more aggressive corrosion between the coating and substrate (including red rusting) as well as faster corrosion within the coating itself. It is therefore critical to have a deposit with uniform thickness **as well as uniform composition** to be considered for fastener applications.

Figure 24: Plated fasteners before and after ASTM B117 testing: Zn-Ni acid PP (left) and Zn-Ni alkaline PP (right). All Zn-Ni acid fasteners showed red rust formation after ~700 h, independent of scribing.

Finally, a benchmark commercial Zn-Ni alkaline plating system – Dipsol America IZ-C17 (LHE Zn-Ni alkaline) – was also examined for salt-spray corrosion performance (ASTM B117). This system has been known to have enhanced HE and HRE performance, but high porosity which can lead to reduced mechanical performance. Using standard plating conditions (current density between 30-60 mA/cm^2, ~52% efficiency, and 0.46 μm/min), initial test plates with the system possessed a composition of 15 wt.% Ni. These parameters were confirmed by Dipsol America. It is worth noting that, at this composition, the coating may be effective because its nobility is much closer to that of the steel substrate. Figure 25 displays the pre- and post-compression test samples plated using pulse-reversing and converted using the trivalent chromium system. In these cases, the uniformity of conversion coat coloration was greater. It was shown that PP and PR waveforms with this electrochemical system produced a coating that, when compromised e.g. by scribing, did not accelerate corrosion of the steel substrate; in fact, this system lead to the best overall corrosion properties, i.e. minimal white rust after 1000 hours.

Figure 25: Scribed pulse-reverse plated samples using the Dipsol alkaline system, before and after 1000 h of exposure. Left set: corrosion plaques with minimal white rust formation beginning at ~800 h. Right set: fasteners, both displaying minimal white rusting, independent of scribing.

5.4   WEAR – PIN-ON-DISC FRICTION

Sliding wear (i.e. Pin-on-Disc friction) testing followed ASTM G99 and was completed using a Tribometer. Testing was initially performed on a 1 inch^2 piece of coated mild steel sample with a wear track diameters of 8 mm (for a 2 m sliding distance) and 10 mm (for a 100 m sliding distance) in order to obtain friction coefficients over short and long sliding wear distances.

Table 4 presents the test results for the Phase I down-selected Zn-based alloys and their respective waveforms. These results were obtained by taking an average of the mean values from three test trials (see Appendix B, Section 10.1). Overall, the Phase II results were very similar to those obtained in Phase I: for example, pulsing plating (refined grain structure) led to lower wear/friction than direct current and values obtained for the Zn-Ni alkaline system were higher than those for Zn-Ni acid. However, it is important to note that the coefficient of friction measured from pin-on-disc testing depends on a number of factors, all of which should be considered to explain the range of values obtained. For example, many factors influence the friction behavior such as humidity, temperature, time to testing (i.e. oxide formation), and condition of the pin/ball. However, in general the Phase II results for the sliding friction correspond reasonably with the coefficient of friction values obtained in torque-tension testing (Section 5.5). The friction values were generally higher for the longer sliding distance due to wear track formation during testing.

Samples from the Dipsol system were also made to compare deposits produced using DC, PP, and PR waveforms. The results showed that mean sliding friction values were within a close range of each other, i.e. spanning from 0.10 to 0.14. Finally, Zn-Ni alkaline samples with the Sol-Gel coating (outlined in Section 4.2.5) were tested, and they showed similar low sliding wear and friction as the metallic coating. However, the difference between the minimum and maximum values was large (see Appendix B, Section 10.1): over a 2 m wear track, for example, while the *mean* friction coefficient was 0.27, the minimum was 0.13 and maximum was 0.49, suggesting rapid breakdown of the polymer during testing.

Table 4: Summary of pin-on-disc results for Phase I down-selected Zn-based alloys.

Alloy	Electrical Waveform Optimized	Coefficient of Friction (Sliding)	
		2m	100m
Cadmium*	DC	0.19	0.49
Zn-Ni alkaline (Atotech)	DC	0.32 (Cr^{3+}) 0.20 (Cr^{6+})	0.55 (Cr^{3+}) 0.35 (Cr^{6+})
	PP	0.13 (Cr^{3+}) 0.15 (Cr^{6+})	0.24 (Cr^{3+}) 0.26 (Cr^{6+})
Zn-Ni alkaline (Dipsol)	DC	0.10 (Cr^{3+})	0.47 (Cr^{3+})
	PP	0.14 (Cr^{3+})	0.34 (Cr^{3+})
	PR	0.12 (Cr^{3+})	0.32 (Cr^{3+})
	PR+Sol Gel	0.27	0.55
Zn-Ni acid	PP	0.09 (Cr^{3+}) 0.12 (Cr^{6+})	0.23 (Cr^{3+}) 0.14 (Cr^{6+})
	PR	0.13 (Cr^{3+}) 0.20 (Cr^{3+})	0.23 (Cr^{3+}) 0.15 (Cr^{6+})
Zn-Ni-Co acid	PP	0.13 (Cr^{3+})	0.15 (Cr^{3+})
	PR	0.16 (Cr^{3+})	0.49 (Cr^{3+})

* Values for Cadmium were obtained from Phase I results.

5.5   TORQUE-TENSION

Using a Skidmore Wilhelm tension instrument in conjunction with a JETCO torque wrench, the torque-tension relationship was determined following the procedure described in the High-Strength Steel Joint Test Protocol (HSS JTP) for Validation of Alternatives to Low Hydrogen Embrittlement Cadmium For High-Strength Steel Landing Gear and Component Applications (07/31/2003, prepared by The Boeing Company, Seattle WA), Section 3.4.2, for high strength steel fasteners. This included a) the use of Grade 9, 1/2"-13 UNC bolts, and b) a Rogard Lube 200 lubricant as well as that per SAE AMS 2518. A Cr^{3+} conversion coating was also applied to test specimens to mirror the Cadmium benchmark. Table 5 summarizes the friction coefficients measured for the three Phase I down-selected alloys. See Appendix B, Section 10.2 for further detail.

Overall, the use of pulse deposition techniques appears to reduce the friction coefficient over that produced using DC approaches. This agrees with the typical increase in hardness, reduction in grain size, and improvement in wear resistant achievable with pulsed metal electrodeposition. In the case of Zn-Ni alkaline (Atotech), the PP friction coefficient (0.15) approaches closest the value possessed by Cadmium (0.12), followed by PP Zn-Ni acid and pulsed Zn-Ni-Co coatings. A similar contrast was observed in the Dipsol Zn-Ni alkaline bath, where the friction coefficient decreased with pulsing waveforms, independent of coating thickness. For example, measured values for PP were 0.16, 0.28, 0.17, and 0.15, while those for DC were 0.30, 0.31, 0.34, 0.32, and 0.16 (outliers may exist due to random error). These results demonstrate benefits of using pulsing waveforms.

Table 5: Summary of torque-tension results for down-selected Zn-based alloys.

Alloy	Electrical Waveform Optimized	Friction Coefficient	
		Phase II.1	**Phase II.2**
Cadmium	DC	**0.12***	
Zn-Ni alkaline (Atotech)	DC	**0.17***	
	PP	**0.15***	
Zn-Ni alkaline (Dipsol)	DC		**0.29 ± 0.07[†]**
	PP		**0.19 ± 0.06[†]**
	PR		**0.24 ± 0.08[†]**
	PR+Sol Gel		**0.19 ± 0.03[†]**
Zn-Ni acid	DC	**0.21***	
	PP	**0.17***	
Zn-Ni-Co acid	DC	**0.21**	
	PP	**0.15**	
	PR	**0.18**	

*-Value obtained during Phase I (see Table 1)
[†]-Value averaged over 3-5 test trials

Again linking hardness and wear resistance, the hardness values of the Zn-Ni alloy coatings produced in the Dipsol bath using pulsing (PP: 493 ± 17 VHN; PR: 500 ± 15 VHN) were slightly higher than the standard for DC (maximum of 450 VHN as outlined in the TDS). However, the coating was notably brittle as indicated by the existence of cracks surrounding the microhardness indentations (Figure 26).
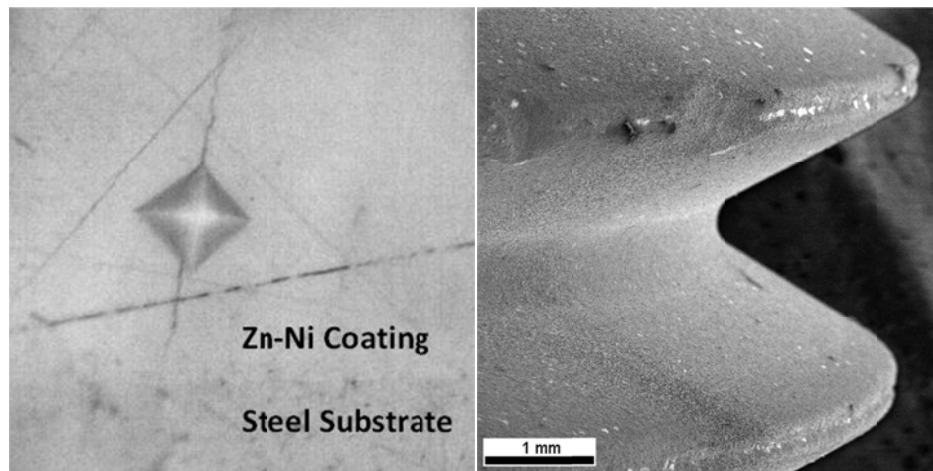
Figure 26: Microhardness indentation taken in pulse-plated Zn-Ni coating in Dipsol bath, illustrating low ductility. Also shown is an SEM image taken of a pulse-plated steel fastener from the same bath.

Finally, the use of a Sol-Gel top coat, as an alternative to the chromate or chromium conversion coatings, also offered good friction properties: fasteners PR-plated using the Zn-Ni alkaline system, then Sol-Gel coated, also reached a friction coefficient of ~0.19. These results, together with those from pin-on-disc testing, suggest that pulsed waveforms in alkaline baths lead to reduced friction coefficients.

5.6   HYDROGEN RE-EMBRITTLEMENT (HRE) – ASTM F519
For this test, 4340 HSS ASTM F519 type 1a1 notched tensile bar were plated and sent to Omega Research Inc. (Justin, TX) for testing, similar to the case for HE testing (see Section 5.2). Again, all plated notched tensile bars were given a bake-out treatment before testing using the standard condition

(191°C for 24 h). Each sample was loaded to a value of 45% NFS and sustained up to 150 hours in a 3.5 wt.% NaCl environment; failure to hold for less than 150 hours was considered a failure. There were three iterations in HRE testing. The first (Phase II.1) was conducted on un-converted samples activated using acidic activation. The second (Phase II.2) focused on sample preparation using conditions recommended by Dipsol America for the LHE Zn-Ni system, i.e. sand blasting and rinsing without acid activation; and complete Cr^{3+} conversion coating application (3 minutes, after Figure 15). The third (Phase II.3) utilized a number of components, including: as a benchmark, plating with the Dipsol America commercial LHE Zn-Ni alkaline plating system; Integran's proprietary techniques applied to the Dipsol system, such as pulse-plating and pulse-reverse plating; and the application of Cr^{3+} conversion coating before bake-out. Table 6 summarizes the results.

Table 6: Summary of ASTM F519 HRE results for down-selected Zn-based alloys.

Alloy	Electrical Waveform Optimized	Phase II.1 Pass/Fail	Phase II.2 Pass/Fail	Phase II.3 Pass/Fail
Cadmium	DC	Marginal PASS[1]		
Zn-Ni alkaline (Atotech)	DC	FAIL[2]	FAIL[3]	
	PP	FAIL[2]	FAIL[3]	
Zn-Ni alkaline (Dipsol)	DC			Marginal PASS[4]
	PP			PASS
	PR			PASS
Zn-Ni acid	DC	FAIL[2]	FAIL[3]	
	PP	FAIL[2]	FAIL[3]	
	PR	FAIL[2]		
Zn-Ni-Co acid	DC	FAIL[2]		
	PP	FAIL[2]		

Notes:
(1)   Failure times of 62, 114, and two greater than 150 hours
(2)   Failure times were all under 4 minutes
(3)   Failure times averaged ~100 minutes for acid and alkaline PP, ~12 minutes for DC
(4)   Using Dipsol-confirmed composition, structure, and plating rate: 1 sample failed at 0.3 hours, while remaining samples exceeded time of 150 hours

These results indicate that the use of acid activation leads to nearly immediate re-embrittlement failure; this is unexpected considering the results in Section 5.2, wherein the same activation procedure did not lead to conventional *embrittlement* failure. Second, the combined use of a physical surface preparation method (sandblasting) and sufficient Cr^{3+} conversion coating led to vastly improved HRE performance of the Zn-based deposits, most so for the bars produced with pulsing waveforms. In particular, the acid PP deposit reached an average failure time of 112 min., and the alkaline PP deposit reached an average failure time of 96 min. On the other hand, the DC plates all failed at a maximum of 26 min. However, these improvements still fell short of the 150 hour target.

In contrast, drastic improvements were obtained in Phase II.3. For example, using the Dipsol commercial bath with standard DC plating conditions, only 1 of 4 samples failed to reach the 150 h mark. Using the Dipsol commercial bath and pulse-plating (PP and PR) conditions, *all samples passed* the 150 h mark. One of the reasons for this improvement is the greater wt.% Ni in the deposit. For example, in order to achieve a low corrosion rate between coating and substrate, the open circuit potential between the two materials should be as close as possible. Additional samples were plated to investigate the role of composition and pulsed-deposition in HRE performance. The results are summarized in Table 7. These results show that HRE failure of both DC and pulsed deposits is closely linked with low wt.% Ni in those deposits. Therefore, as pulsing waveforms produce a deposit with heightened wt.% Ni (e.g. Figure 13) – *as well as the desirable single γ-phase microstructure as shown in Phase I* – they can provide a greater

HRE-coating than DC plating in a given bath. It's worth noting that the compositions measured in Table 7 are within the 12-18% range outlined in the TDS for the Dipsol bath.

Table 7: Detailed summary of ASTM F519 HRE results for Dipsol bath plating conditions.

E	Run Numbers	Composition	Pass/Fail
DC	10-ZNID-J0015, 0016	15.7 – 15.9 wt.% Ni[1]	**Marginal PASS**[2]
	10-ZNID-J0087	12.5 wt.% Ni	**FAIL**[3]
	10-ZNID-XJ159,160	12.2 wt.% Ni	**FAIL**[3]
PP	10-ZNID-J0017, 0018	15.1 – 15.9 wt.% Ni[1]	**PASS**
	10-ZNID-XJ162,163	12.3 wt.% Ni	**FAIL**[3]
PR	10-ZNID-J0033, 0037	15.3 – 16.1 wt.% Ni[1]	**PASS**
	10-ZNID-XJ126, 127 10-ZNID-XJ136, 137	13.9 – 14.3 wt.% Ni[1] 15.7 wt.% Ni	**PASS**

Notes: (1) – HRE bar composition was not measured; instead, compositions of test plates before and after HRE bar plating are given to establish a range
(2) – 1 sample failed at 0.3 hours, while remaining samples exceeded time of 150 hours
(3) – Failure times of under 0.3 hours were recorded for all four HRE bars

The influence of the Sol-Gel coating, as a replacement to the chromate or chromium conversion coating, was also determined. In this case, type 1a1 bars were PR plated using the Zn-Ni alkaline system (Dipsol), then Sol-Gel coated. Figure 27 presents a typical 1a1 bar; all Sol-Gel coated bars passed re-embrittlement testing.
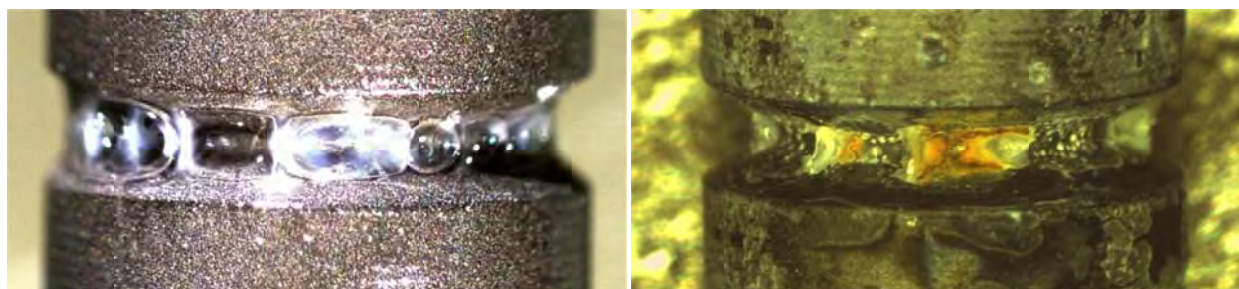
Figure 27: Notch of Sol-Gel coated F519 type 1a1 bar. Coating left air bubbles in notch. Also shown: Sol-Gel coated F519 type 1a1 bar after HRE testing, showing degradation (but passing) of the coating.

5.7   **POTENTIO-DYNAMIC CORROSION TESTING**
Early HRE failure may be caused by a number of factors, one of the more significant being composition of the Zn-Ni coating. More specifically, the composition of the Zn-Ni alloy (i.e. wt.% Ni) directly influences the corrosion potential of the coating which can have a significant effect on the strength of the galvanic couple with the steel substrate. In the initial potentio-dynamic corrosion testing in this project, the benchmark coating (Cadmium) had a reference potential of approximately –0.7 V; this is just below (less noble) than that of the steel substrate. Therefore, in order to minimize the driving force for galvanic corrosion – while maintaining the sacrificial nature of the coating – a very similar potential to Cadmium is a target for the Zn-Ni system. In Phase II, potentio-dynamic polarization test results illustrate that the potential of Integran's pulse-plated and pulse-reverse plated coatings do increase with wt.% Ni, and in some cases match the potential of Cadmium (Figure 28). In particular, the subset of coatings with a composition of ≥15 wt.% Ni was found to be nearly constant at approximately –0.7V.
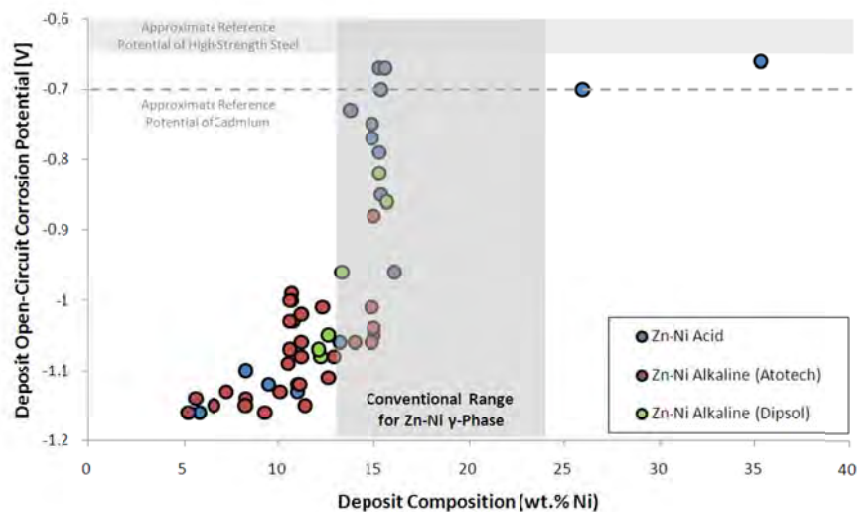
Figure 28: Measured corrosion potential versus Zn-Ni deposit composition for acid and alkaline deposits. Conventional Zn-Ni single γ-phase is outlined using the Zn-Ni phase diagram.

Based on a benefit demonstrated using pulsing electrical waveforms, i.e. higher Ni contents, Integran's approach can also produce suitable Zn-Ni coatings for corrosion and HRE performance.

6.0   TASK 8 – COMPREHENSIVE COATING PERFORMANCE EVALUATION

6.1   TASK OBJECTIVES
The objective of Task 8 was to evaluate for high-strength steels the general performance of selected nanoscale Zn-based coating systems relative to current Cd-plating processes. Using the performance results from the five test methods outlined in Task 7, the Zn-Ni coatings can be considered with respect to the performance of Cadmium.

6.2   EVALUATION OF COATINGS
Below is a brief summary and recapitulation of the results obtained in Task 7.

6.2.1   Hydrogen Embrittlement (HE)
Overall, most plating systems passed this requirement, meeting that for the Cadmium system. Systems not passing HE testing, namely the pulse-reverse Zn-Ni acid and Zn-Ni-Co, may possess large *changes* in plating inefficiencies in plating resulting in hydrogen generation and residual in the steel substrate not removed during the bake-out step. The addition of a chromate or chromium conversion coating did not appear to influence the overall results.

6.2.2   Salt Spray Corrosion
Most plating systems passed this test and did not produce red rust, either in the un-scribed or scribed condition. In the un-scribed condition, one system which did demonstrate red rusting was the Zn-Ni-Co. The likely cause of this failure is the combination of a high level of Ni+Co: XRF measured a composition of Zn-11.6 wt.%Ni-3.4 wt.%Fe. This level of Ni+Co likely increases the nobility of the deposit to the extent that it no longer provides sacrificial protection to the steel. However, the generation of red rust in this sample occurred only in the un-converted condition: a second sample with Zn-11.6 wt.%Ni-3.1 wt.%Co, and converted using the Atotech trivalent chromium coating, did not demonstrate red rusting after 1000 hours of salt spray exposure. Therefore, design of a suitable alloy composition, as well as the selection of a suitable conversion coating, enhances the corrosion performance of the deposit.

In general, samples possessing conversion coatings (in the Cr^{6+}, and more so in the Cr^{3+} form) performed drastically better than their un-converted counterparts. In addition, in some cases (e.g. acid baths using pulsing waveforms, and the Dipsol alkaline bath using pulsing waveforms) the generation of white rust was delayed until times similar to the Cadmium system, i.e. >1000 hours. The conversion coating in many cases introduced a color gradient on the panel which may be related to a number of factors. In specific, it may be due to including insufficient rinsing, temperature variation in rinsing, conversion thickness variations, localized Zn-Ni deposit thickness and/or composition, or even localized substrate variations. It was considered that the rusting uniformity and time to formation may be related to the gradient of coloration found on the panels following conversion. However, conclusions could not be drawn from the present project as there were inconsistent results between panels which overall had a wide range of deposit characteristics.

Aside from the influence of a conversion coating, pulsing deposition waveforms also influence the corrosion response of the coating. In particular, in polycrystalline metal coatings, localized attack and pitting will occur where the grain boundaries intersect the corroding free surface [24]. While nanocrystalline metals have an increased grain boundary volume fraction and may exhibit increased uniform corrosion rates, they also have superior pitting corrosion resistance when compared to their polycrystalline counterparts [25]. This pitting resistance has been attributed to a more defective passive layer which increases the uniformity of corrosive attack [25], an issue which would be important for high-strength steel fasteners.

Signs of the effect of grain size reduction may be observed from the salt spray corrosion results in this work, i.e. comparing DC and PP Zn-Ni alkaline deposits with and without conversion coatings (Figure 29). In the case of samples without a conversion coating, it appeared that the deposit produced through pulse plating promoted a more uniform distribution of white rusting, albeit with a similar amount as the DC-plated sample. In the case of samples with the trivalent chromium conversion coating, a clear difference was seen between the two samples: the DC sample possessed significant white rusting, whereas the PP sample possessed minimal white rusting. This may be due to the reduced grain size of the deposit. In addition, this improved performance may be due to the increased nobility (i.e. higher wt.% Ni) of the deposit – **a result of pulsing waveforms throughout all systems studied**. Furthermore, this improved performance may be due to an increased effectiveness of the conversion coating on a deposit with reduced grain size, although this may be less likely as the surface coloration of the DC and PP converted pieces looked similar (Figure 29).
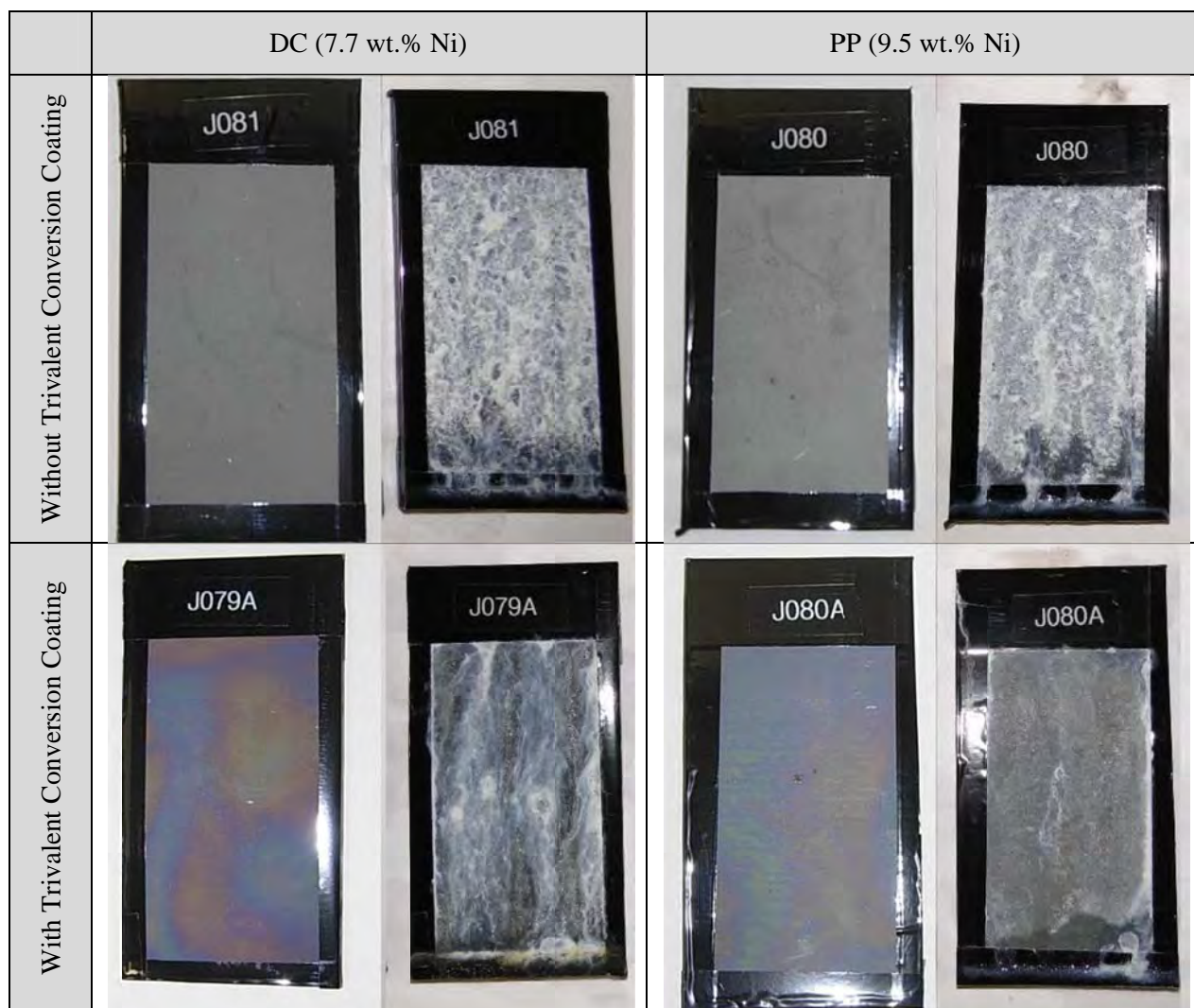
Figure 29: Comparison of Phase II.1 Zn-Ni deposits produced from the Atotech alkaline bath, before and after 1000-hour salt-spray corrosion testing.

6.2.3   Sliding Wear / Pin-on-Disc Friction

In the sliding wear test set-up, it was found that the friction coefficient of the Zn-Ni coatings was comparable to that for the Cadmium coating. In the case of the 2 m wear length sliding wear length, the Cadmium friction coefficient measured was 0.19.   For the Zn-Ni coatings produced using pulsing waveforms (both acid and alkaline), the friction coefficients approached that of cadmium and surpassed that for conventional DC waveforms. Both the hex chromate and trivalent chromium conversion coatings appeared to provide similar results, suggesting the more environmentally-benign trivalent chromium conversion coating is suitable for use on high-strength fasteners. As the track length was increased to 100 m, again the Zn-Ni acid and alkaline baths with pulsed waveforms possessed the best overall (and similar) results compared to the value of 0.49 measured for Cadmium. Overall, the values suggest that the friction coefficients of select Zn-Ni coatings can be designed using pulsing waveforms to be near that for Cadmium by engineering/refining the grain structure. It was also found that the use of a unique Sol-Gel conversion coating alternative can offer similar low sliding wear properties.

6.2.4   Torque-Tension

Similar to the case of Taber Wear / Pin-on-Disc testing, it was determined that the friction coefficients obtained for the Zn-Ni systems are similar (albeit slightly larger) to that for a Cadmium deposit. The best results measured were from the Zn-Ni alkaline systems using pulse plating and pulse-reverse plating waveforms: in the most significant case, the Dipsol DC-plated fasteners had friction coefficients nearly twice that of those using pulsing waveforms, with the lower values being attributed to the smoother surface and finer grain structure. Similarly, increased friction was found in the Zn-Ni acid system using DC waveforms over pulsed waveforms. Although these results and those from pin-on-disc can be influenced by sample preparation and test environment (e.g. existence and coverage of lubricant, environmental state at the time of testing), together the results from these friction tests suggest that improved wear can be achieved using pulse plating techniques.

6.2.5   Hydrogen Re-Embrittlement (HRE)

Hydrogen re-embrittlement testing has been considered a critical measure for fastener applications. While the Cadmium-plated bars (2 of the 4) were shown to last up to the 150-hour goal, success for the Zn-Ni coatings required a number of iterations in order to achieve a coating that could successfully pass the HRE test, which identified the importance of surface activation methods as well as optimal coating characteristics, Through the iterative analysis, the most promising conditions were Integran's pulse plating and pulse-reverse plating waveforms with the commercial LHE Zn-Ni alkaline system (Dipsol). In particular, pulsing waveforms can produce 1) a deposit with heightened wt.% Ni, better matching the open circuit potential of the underlying substrate, and 2) a dense deposit with the desirable single γ-phase microstructure for heightened corrosion uniformity – and thereby provide a greater HRE-coating than DC plating in a given bath. It was also found that sample preparation and chromating application played a measurable role in the overall performance of notched bars. It was also determined that an alternative Sol-Gel coating can be used as a suitable replacement for conversion coatings (trivalent or otherwise) to aid in low-friction as well as maintain the hydrogen re-embrittlement performance of high-strength steel fasteners.

7.0   TASK 9 – BARREL/TANK/RACK PLATING EVALUATION

7.1   TASK OBJECTIVES

The objective of Task 9 was to investigate the compatibility of the selected processes with conventional production plating techniques, such as high volume barrel plating.

7.2   EVALUATION OF BARREL PLATING

Barrel plating was attempted primarily in the Zn-Ni alkaline systems. The barrel plating apparatus is shown in Figure 30. It was determined that two hundred (200) 1/4"-20, 3/4"-long Grade 5 steel fasteners could be DC plated, *as well as pulse-plated*, the latter producing dense and bright coatings on the fasteners over the surface of the "valley" of the thread (Figure 31).
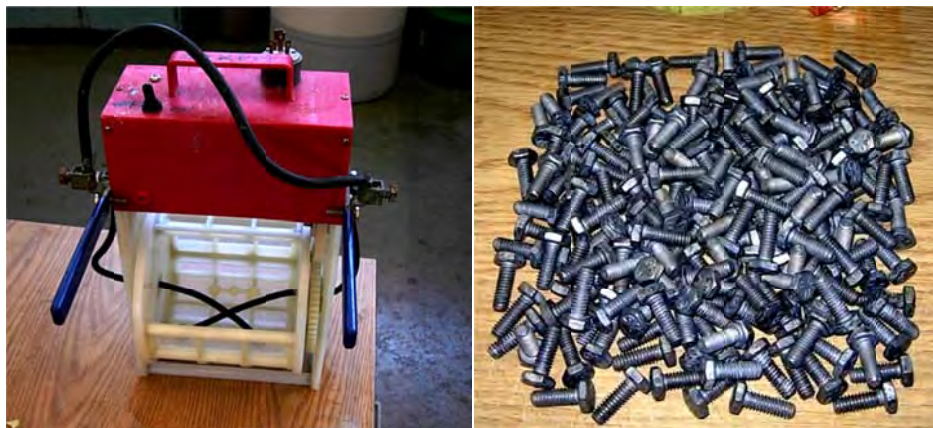
Figure 30: Barrel plating apparatus for 40-L plating tanks. Also shown are 200 fasteners coated with a single homogenous layer of ZnNi with uniform alloy composition using Integran's pulsed electrical waveform.
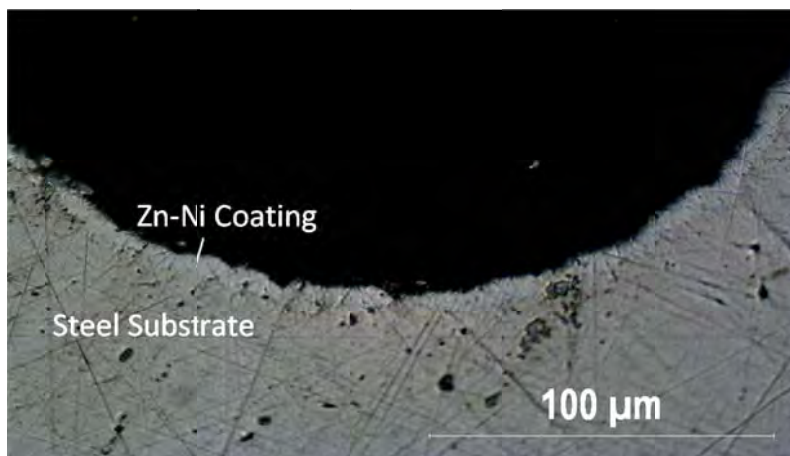
Figure 31: Cross-section of barrel-plated fastener using a pulsed waveform and alkaline bath chemistry.

During barrel plating, one of the key differences is the constant mixing of air into the bath during the rotation of the barrel. As the alkaline plating bath becomes less efficient with exposure to air (a result of carbon dioxide leading to production of Na_2CO_3), barrel plating requires additional monitoring to ensure carbonate levels remain low. At levels high enough, a percentage dilution and replenishment serves to return to the bath to operation.

Finally, thickness uniformity may be considered to change between rack and barrel plating set-ups. While the thickness profile in a rack-type set-up can lead to thickness variations on parts with sharp geometries (e.g. Figure 13 and Figure 14), the composition uniformity plays a large role in the overall corrosion response of the part. In particular, parts with local composition non-uniformities may experience localized galvanic coupling, leading to self-directed breakdown of the protective coating. However, as shown in the present work, pulse-plating electrical waveforms can not only produce microstructures with refined grains, these waveforms can be used in barrel plating set-ups to aid in more compositionally-uniform deposits.

8.0   CONCLUSIONS

The focus of this project was to develop a nanostructured Zn-based alloy coating suitable for Cd-replacement on high strength steel fasteners. Phase I evaluated the relationship between coating microstructure and material properties (relevant for fastener applications) in order to develop an optimal <u>microstructurally designed Cd-replacement coating.</u> The results from Phase I revealed that fine grained structures produced via pulse plating from modified commercial Zn-alloy plating solutions had some significant benefits over conventional DC plating, including:

    1) bright, uniform, dense microstructure,
    2) uniform, equiaxed grain size throughout thickness of the coating,
    3) increased microhardness,
    4) single γ-phase crystallographic microstructure (in the case of Zn-Ni),
    5) increased corrosion resistance compared to other Zn-Ni alloys,
    6) decreased friction (torque-tension), and
    7) passing the ASTM F519 hydrogen embrittlement (HE) testing (even with a dense microstructure, i.e. without porosity).

The benefits of pulse plating on the performance of Zn-alloys are expected to provide superior coating properties similar or superior to Cd and essential to high strength steel fasteners.

Phase II performed in-depth analysis and testing of the alloy systems and plating chemistries used down-selected from Phase I (Alkaline and Acid ZnNi, ZnNiCo). At the conclusion of the program, the alkaline ZnNi plating system supplied by Dipsol of America, provided the best combination of properties for Cd-alternative applications.

The use of optimized pulsed plating parameters to synthesize Zn-Ni alloys produced using the commercial alkaline chemistry was found to:

- Possess similar properties as the conventional Cadmium coatings, such as wear, embrittlement, and in-service re-embrittlement;
- Refine the microstructure to result in fully dense coating with higher hardness, greater wear resistance, lower friction, and greater corrosion protection against direct-current counterparts;
- Provide improved deposit composition uniformity, higher Nickel content coatings, and single-phase γ microstructure, which can improve corrosion protection as well as hydrogen (a.k.a. in-service) re-embrittlement;
- Reduce deposit porosity, which can improve wear resistance, lower friction coefficients, and provide improved aesthetics;
- Provide scalable process methods to reach high outputs, i.e. barrel plating, and can be integrated into existing manufacturing lines.

Together, the results in this report show that Integran's waveform engineering approach provides additional benefit over conventional DC plating and can be successfully integrated into a commercial scale as a potential swap-out technology with current Cadmium-plating systems.

9.0   APPENDIX A – SUMMARY OF PHASE I WORK PERFORMED AND RESULTS

9.1   PHASE I DEVELOPMENT OF NANOSTRUCTURED ZN-NI AND ZN-NI-CO ALLOYS

After searching the academic literature and contacting several commercial Zn-Ni suppliers, an acid and a number of alkaline solutions were selected for investigation, including:

1. Zincrolyte® CLZ-Ni 6340 Bright Zn-Ni alloy (proprietary acid process from Enthone)
2. Dipsol IZ 250Y (proprietary alkaline Bright Zn-Ni process from Dipsol of America)
3. ReflectAlloy ZNA® (proprietary alkaline Zn-Ni from Atotech)
4. PG ZN (non-proprietary solution from the academic literature)

During the Phase I work, the screening procedure used for assessment of the various Zn-Ni plating solutions consisted of three stages: Hull Cell investigation, Beaker Studies, and Tank Plating. Hull cells provide quick information on the effects of applied waveform, duty cycle, and frequency, on coating quality with respect to general coating integrity, composition uniformity and microstructure. Beaker plating further tested the deposit properties with respect to flow, cathode/anode placement, and current distribution on physical properties such as microhardness, composition, crystal structure, and deposition efficiency.

9.1.1   Zincrolyte® CLZ-Ni 6340 Bright Zn-Ni alloy

The preliminary Hull cell results with this acid process were very promising. The system responded very well to pulse plating. The coatings were found to have good coating integrity (no cracking, spalling, or blistering) and changes in the pulse conditions resulted in significant changes to the grain size and texture of the material. In most cases, the composition of the coating was higher than that specified in the technical data sheet for the process (5-9 wt.% Ni). Previous studies with electrodeposited Zn-Ni identify an optimal Ni range between 14-16 wt.% with a single γ-phase crystal structure for optimal corrosion resistance.

The results from the Hull cell tests were used to select a narrower set of operating conditions for another DOE using a 2L beaker. However, it was determined that pulsing quickly degraded the organic brighteners in the solution, creating instability. As a result, a new solution was mixed without adding the organic brighteners. Upon completion of the Phase I DoE it was determined that <u>PP could be used to obtain a bright coating with a seemingly dense microstructure, even in the absence of organic brighteners in the solution</u>. An optimal set of operating conditions were identified that produced fine-grained, bright deposits with the desired wt.% Ni.

9.1.2   Dipsol IZ 250Y Bright Zinc-Nickel PLUS

During Phase I, numerous difficulties were encountered with the Dipsol Zn-Ni system. The Hull cell tests performed with this solution were plagued with solution stability issues. The solution also produced a large amount of bubbling during plating, indicating a relatively poor efficiency (leading to very low plating rate). Due to the low plating rate, very little information was obtained beyond identifying the presence of the γ-phase. However, due to the relatively small volume of the Hull cell, it was possible large changes in the solution chemistry occurred during the run, leading to the poor results. In addition, during Phase I there was limited availability of the stock IZ-250Y solution from the Canadian supplier; thus, this bath was not investigated further. In Phase II, effort was therefore made to obtain the low hydrogen embrittlement (LHE) Zn-Ni IZ-C17 solution directly from the Dipsol representative in the United States.

9.1.3   ReflectAlloy ZNA®

The Atotech ReflectAlloy solution progressed immediately to 2L beaker scale testing during Phase I. One of the four available make-up recipes provided by Atotech was selected for plating, namely the

'Technical Finish' Zn-Ni bath with NaOH as a chemical base. A first DoE was performed using plating waveforms successful in the Enthone Zn-Ni solution; however, these resulted in a dull coating with various shades of grey matte color. A second and broader DoE was conducted in order to identify an optimal plating condition for pulse plating. Some conditions were found which produced coatings that were shiny and uniform, although high current density areas tended to produce somewhat rough coatings. Deposits produced during the second DoE were further investigated for composition using a SEM with EDX, microstructure using an XRD, grain size, and microhardness. After completion of the DoEs, an optimal condition was selected that produced semi-bright, uniform deposits, and possessed desirable physical characteristics.

This bath had particular sensitivity to additive replenishment due to the operating conditions inherent in using an inert anode. Due to this sensitivity, only limited pulse-plating conditions were identified which could maintain bath chemistry and plating behaviour; it was decided during Phase I that time would be used better in further developing other alloy systems and conditions. In addition, high flow was required during plating for uniform deposits; on the other hand, high flow can increase the interaction between the ambient air and the solution, forming $NaCO_3$, decreasing coating quality, and compromising plating efficiency.

9.1.4 PG ZN Alkaline Zn-Ni
Hull cell testing followed the same DoE as used for the Enthrone acid solution, including a number of pulse plating variables. However, these variables were found to have less impact on the composition and microstructure than observed with the Enthone system. The deposits were found to be of relatively good quality (no visible cracks, blistering, or spalling) and the composition range was found to be in the range of single γ-phase with little variation between pulsing conditions. The deposit was primarily dull in the lower current density regions, semi-bright at medium current density areas, and burnt at the high current density edges. The solution was found to have poorer covering power and throw relative to the Enthone solution, but this could be reduced somewhat with some pulse plating conditions.

Based on the Hull cell results, a narrower set of conditions was identified and samples were produced in a 2L beaker. Initial tests revealed that the solution flow had a significant effect on the quality of the deposit. While low flow conditions yielded deposits similar to that obtained in the Hull cell, higher flow significantly degraded the deposit. In addition, the solution was found to be relatively unstable and large changes in temperature and pH were found to occur during each run. As a result of these issues, further investigation of the PG Zn-Ni solution was abandoned.

9.1.5 Zn-Ni-Co System
In order to investigate a possible ternary solution, a Zn-Ni-Co alloy bath chemistry was developed by adding a source of Co to the acid Zn-Ni bath. The operating conditions were primarily that of the Zn-Ni acid bath, which comprised the majority of the bath chemistry. Optimal conditions identified for use with the Zn-Ni bath were applied to the Zn-Ni-Co bath to confirm its operation, stability, and quality of deposit. These conditions were successful in producing a uniform, bright deposit for DC and pulse plating electrical waveforms. The bath had no apparent sensitivity and was considered stable in operation. All conditions were investigated for composition using a SEM with EDX, microstructure using an XRD to determine crystal structure and grain size, and microhardness. Deposits were uniform and fully-dense, and had good coating integrity and appearance (no cracking, blistering, pitting, or nodules). The composition of wt.% Co and Ni could be further tailored using refined pulse plating electrical waveforms, proving beneficial for reaching the single γ-phase and target nobility.

9.2 SCORING AND DOWN-SELECTION OF PHASE I SYSTEMS FOR PHASE II WORK
In order to narrow down the potential Cd-replacement alternatives, a decision making matrix was formed to determine the top three optimal conditions to be evaluated more closely in Phase II. Selection criteria

were separated into three different categories: Process, Characterization, and Properties. The criteria to evaluate each system and condition are explained below, with assigned weights.

9.2.1   Process – 30%
The process parameter is related to the bath operation and sample production. The process category was subdivided into the following six subcategories:

- **Plating rate** (weight of 5%) – The higher the plating rate, the better to ensure that if employed in industry the production time would be reduced.
- **Current efficiency** (weight of 7.5%) – Efficiency is related to hydrogen evolution during the plating process, and thus the higher the efficiency the lower the amount of hydrogen produced and the lower the chances of HE occurring.
- **Thickness uniformity** (weight of 5%) – Thickness consistency over the entire bolt is important to ensure a uniform coating. Cd coatings are uniform on bolts, and therefore the replacement for Cd should also be somewhat uniform to mimic operational parameters such as torque-tension.
- **Compositional uniformity** (weight of 5%) – Cd is compositionally uniform and, since many properties rely on composition to determine their performance, a uniform coating ensures that no localized variance occurs between the hills and valleys on the threads of the bolts.
- **Bath stability** (weight of 5%) – The stability of the bath is an important parameter when evaluating its operation. Bath stability is related to any changes that occur as a result of plating, such as the color change witnessed in the Zn-Fe bath, that is not the result of any chemical alterations to the bath.
- **Bath sensitivity** (weight of 2.5%) – The sensitivity of the bath to changing pH and temperature is of interest to evaluate. However, the weight assigned to bath sensitivity is only 2.5% because there are instruments that can be employed to ensure the bath is within operating conditions to avoid issues.

9.2.2   Characterization – 10%
The characterization category is related to the integrity of the sample, independent of its performance on installation requirements. These parameters, save for grain size, seem to have no effect on the performance parameters outlined in the next section, and therefore are assigned a low importance. The characterization category is subdivided into the following subcategories:

- **Grain size** (weight of 2.5%) – The smaller the grain size of the sample, the more superior its physical properties, such as corrosion resistance, hardness, and coefficient of friction. Thus, grain size is an important parameter, but it is assigned a small weight due to the higher weight placed on the actual performance of the coating.
- **Crystallographic Phase** (weight of 2.5%) – The phase of the coating is directly related to its corrosion resistance, and thus has an assigned weight of 2.5%. A single phase coating is more corrosion resistant than a multi-phase coating.
- **Morphology** (weight of 2.5%) – Surface morphology is thought to be related to HE and HRE. However, the actual results of the performance testing are more conclusive and thus the weighting assigned to surface morphology is only 2.5%.
- **Coating integrity** (weight of 2.5%) - Otherwise referred to as appearance, coating integrity is important in end-product assessment, but has little relevance to coating properties unless pits, nodules, or dendrites are formed. Thus, a low weighting of 2.5% is assigned to this subcategory. Good coating integrity refers to no pits, nodules, or dendrites, and a shiny, uniform coating.

9.2.3   Properties – 60%
The property parameters are related to the mandatory characteristics of the coating during installation in

lieu of Cd. The following subcategories were used for evaluation:

- **Hardness** (weight 5%) – Hardness is a relatively important characteristic as it might affect coating coefficient of friction, and therefore the assigned weighting is 5%. The harder the sample, the more likely it is nanostructured and will have a good coefficient of friction.
- **Ductility** (weight of 10%) – Coating ductility is assumed to be related to HRE and thus is assigned a weighting of 10%. If the coating is ductile, then it will not crack in the notch of the Type 1a.1 bars and has a higher chance of passing HRE testing.

Deemed to be the most important coating characteristics to high strength steel fasteners are corrosion resistance, HE and friction. Cd has excellence performance in all three of these areas.

- **Coefficient of friction** and the related **torque-tension relationship** (weight of 15%) – These performance criteria are important for high strength steel fasteners to ensure repeatability of tension after a specific torque is applied during installation. It is also important that the coefficient of friction be similar to that of Cd, and therefore the assigned weighting is 15%.
- **Corrosion resistance** (weight of 15%) – Corrosion resistance is also a critical requirement for high strength steel fasteners in service, and therefore was assigned a weight of 15%.
- **Hydrogen Embrittlement** (weight of 15%) – HE is absolutely critical to the intended application as fasteners cannot be used if the coating is embrittling, and thus the assigned weight was also 15%.

Table 8 below outlines the scoring matrix criteria with the respective quantitative weightings.

Table 8: Criteria to evaluate each Zn alloy candidate system with respective weightings.

Criteria	Quantitative Weight (%)
Process	
Plating Rate	5
Current Efficiency	7.5
Thickness Uniformity	5
Compositional Uniformity	5
Bath Stability	5
Operating Conditions	2.5
Characterization	
Grain Size	2.5
Phase	2.5
Morphology	2.5
Integrity	2.5
Properties	
Hardness	5
Ductility	10
Friction	15
Corrosion	15
HE	15
TOTAL	100

Using the above criteria, a decision-making matrix was employed to determine the top three best alternative coatings to Cd. The decision-making matrix can be viewed in Table 9. The properties were given higher ratings if they were similar to that of Cd. By evaluating the values obtained from the table, it was discovered that the most promising coatings for Cd-replacement alternatives are:

1. PP-plated Zn-Ni Alkaline (Score = 81%)
2. PR-plated Zn-Ni Acid (Score = 74%)
3. PP-plated Zn-Ni-Co (Score = 74%)

Note: The values that are highlighted in red indicate the condition that performs the best in the category.

Table 9: Summary of the Phase I scoring matrix for all Zn-based alloy candidate systems. This includes Zn-Co, Zn-Fe, and other systems not carried forward from the Phase I work due to lower scoring.

Criteria	wi (%)	ZNNI ALKA DC Cij	Pij	fij	ZNNI ALKA PP Cij	Pij	fij	ZNNI ACID DC Cij	Pij	fij	ZNNI ACID PP Cij	Pij	fij	ZNNI ACID PR Cij	Pij	fij	ZNCO DC Cij	Pij	fij
Process																			
Plating Rate	5	0.59	0.49	2.46	0.36	0.30	1.50	0.62	0.53	2.63	0.46	0.39	1.95	1.18	1.00	5.00	0.68	0.58	2.88
Current Efficiency	7.5	99.00	0.99	7.43	93.00	0.93	6.98	100.00	1.00	7.50	90.00	0.90	6.75	97.00	0.97	7.28	100.00	1.00	7.50
Thickness Uniformity	5	0.54	0.57	2.87	0.94	1.00	5.00	0.76	0.86	4.32	0.29	0.33	1.65	0.31	0.35	1.76	0.77	0.88	4.38
Compositional Uniformity	5	0.84	0.79	3.96	0.92	0.87	4.34	0.55	0.54	2.70	0.74	0.73	3.63	1.02	1.00	5.00	0.54	0.53	2.65
Bath Stability	5	10.00	1.00	5.00	10.00	1.00	5.00	10.00	1.00	5.00	10.00	1.00	5.00	10.00	1.00	5.00	10.00	1.00	5.00
Sensitivity	2.5	7.00	0.70	1.75	7.00	0.70	1.75	7.00	0.70	1.75	7.00	0.70	1.75	7.00	0.70	1.75	6.00	0.60	1.50
	30			23.47			24.56			23.89			20.72			25.79			23.90
Characterization																			
Grain Size	2.5	52.00	0.41	1.03	27.00	0.79	1.98	41.35	0.52	1.29	24.40	0.88	2.19	59.75	0.36	0.90	56.15	0.38	0.95
Phase	2.5	5.00	1.00	2.50	5.00	1.00	2.50	5.00	1.00	2.50	5.00	1.00	2.50	5.00	1.00	2.50	5.00	1.00	2.50
Morphology	2.5	2.00	0.40	1.00	2.00	0.40	1.00	3.00	0.60	1.50	5.00	1.00	2.50	5.00	1.00	2.50	2.00	0.40	1.00
Integrity	2.5	3.00	0.60	1.50	5.00	1.00	2.50	5.00	1.00	2.50	5.00	1.00	2.50	1.00	0.20	0.50	4.00	0.80	2.00
	10			6.03			7.98			7.79			9.69			6.40			6.45
Properties																			
Hardness	5	270.00	0.85	4.27	303.00	0.96	4.79	206.00	0.65	3.26	290.00	0.92	4.59	312.00	0.99	4.94	119.00	0.38	1.88
Ductility	10	0.70	0.07	0.72	0.80	0.08	0.82	9.70	1.00	10.00	1.18	0.12	1.22	4.90	0.51	5.05	0.50	0.05	0.52
Friction	15	0.17	0.82	12.35	0.15	0.93	14.00	0.39	0.36	5.38	0.33	0.42	6.36	0.27	0.52	7.78	0.20	0.70	10.50
Corrosion	15	705.00	0.70	10.46	916.00	0.91	13.59	310.00	0.31	4.60	699.00	0.69	10.37	604.00	0.60	8.96	361.00	0.36	5.36
Hydrogen Embrittlement	15	1.00	1.00	15.00	1.00	1.00	15.00	1.00	1.00	15.00	1.00	1.00	15.00	1.00	1.00	15.00	1.00	1.00	15.00
	60			42.81			48.21			38.24			37.54			41.73			33.25
TOTAL	100			72.30			80.76			69.93			67.96			73.91			63.61

Criteria	wi (%)	ZNCO PP Cij	Pij	fij	ZNCO PR Cij	Pij	fij	ZNFE DC Cij	Pij	fij	ZNFE PP Cij	Pij	fij	ZNIC DC Cij	Pij	fij	ZNIC PP Cij	Pij	fij	ZNIC PR Cij	Pij	fij
Process																						
Plating Rate	5	0.45	0.38	1.91	1.17	0.99	4.96	0.19	0.16	0.81	0.12	0.10	0.51	0.64	0.54	2.71	0.53	0.45	2.25	0.88	0.75	3.73
Current Efficiency	7.5	72.00	0.72	5.40	99.00	0.99	7.43	46.00	0.46	3.45	27.00	0.27	2.03	99.00	0.99	7.43	93.00	0.93	6.98	90.00	0.90	6.75
Thickness Uniformity	5	0.43	0.49	2.44	0.64	0.73	3.64	0.66	0.75	3.75	0.56	0.64	3.18	0.88	1.00	5.00	0.27	0.31	1.53	0.39	0.44	2.22
Compositional Uniformity	5	0.70	0.69	3.43	0.67	0.66	3.28	0.12	0.12	0.59	0.10	0.10	0.49	0.52	0.51	2.55	0.63	0.62	3.09	1.06	0.96	4.81
Bath Stability	5	10.00	1.00	5.00	10.00	1.00	5.00	3.00	0.30	1.50	3.00	0.30	1.50	10.00	1.00	5.00	10.00	1.00	5.00	10.00	1.00	5.00
Sensitivity	2.5	6.00	0.60	1.50	6.00	0.60	1.50	3.00	0.30	0.75	3.00	0.30	0.75	10.00	1.00	2.50	10.00	1.00	2.50	10.00	1.00	2.50
	30			19.68			25.80			10.84			8.46			25.19			21.34			25.01
Characterization																						
Grain Size	2.5	58.00	0.37	0.92	37.40	0.57	1.43	48.00	0.45	1.11	39.45	0.54	1.36	23.20	0.92	2.31	31.75	0.67	1.69	21.40	1.00	2.50
Phase	2.5	5.00	1.00	2.50	2.00	0.40	1.00	5.00	1.00	2.50	5.00	1.00	2.50	2.00	0.40	1.00	2.00	0.40	1.00	2.00	0.40	1.00
Morphology	2.5	2.00	0.40	1.00	2.00	0.40	1.00	2.00	0.40	1.00	2.00	0.40	1.00	5.00	1.00	2.50	3.00	0.60	1.50	5.00	1.00	2.50
Integrity	2.5	4.00	0.80	2.00	5.00	1.00	2.50	4.00	0.80	2.00	4.00	0.80	2.00	4.00	0.80	2.00	3.00	0.60	1.50	3.00	0.60	1.50
	10			6.42			5.93			6.61			6.86			7.81			5.69			7.50
Properties																						
Hardness	5	96.00	0.30	1.52	133.00	0.42	2.10	183.00	0.58	2.90	231.00	0.73	3.66	263.00	0.83	4.16	316.00	1.00	5.00	131.00	0.41	2.07
Ductility	10	1.10	0.11	1.13	0.76	0.08	0.78	0.50	0.05	0.52	0.50	0.05	0.52	1.15	0.12	1.19	0.75	0.08	0.77	6.25	0.64	6.44
Friction	15	0.22	0.64	9.55	0.20	0.70	10.50	0.14	1.00	15.00	0.17	0.82	12.35	0.21	0.67	10.00	0.19	0.74	11.05	0.17	0.82	12.35
Corrosion	15	427.00	0.42	6.34	0.00	0.00	0.00		0.00	0.00		0.00	0.00		0.00	0.00	1011.00	1.00	15.00	1011.00	1.00	15.00
Hydrogen Embrittlement	15	1.00	1.00	15.00	0.00	0.00	0.00	0.00	0.00	0.00		0.00	0.00	1.00	1.00	15.00	1.00	1.00	15.00	0.00	0.00	0.00
	60			33.53			13.39			18.41			31.52			30.35			46.83			35.87
TOTAL	100			59.64			45.12			35.87			46.84			63.34			73.85			68.38

10.0   APPENDIX B – TORQUE-TENSION AND PIN-ON-DISC ANALYSIS

In Sections 5.4 (Pin-on-Disc) and 5.5 (Torque-Tension), analysis was conducted to obtain values of friction coefficients. For Pin-on-Disc testing, ASTM G99 – Standard Test Method for Wear Testing with a Pin-on-Disc Apparatus – was followed. For Torque-Tension testing, the procedure followed the High-Strength Steel Joint Test Protocol (HSS JTP, 07/31/2003) prepared by The Boeing Company (Seattle, WA). This included a) the use of Grade 9, 1/2"-13 UNC bolts, and b) a Rogard Lube 200 lubricant as well as that per SAE AMS 2518. The analyses for each test method – results summarized in Table 4 and Table 5, respectively – are more completely described in this Appendix.

10.1   PIN-ON-DISC ANALYSIS

The work performed in Phase II continued that from Phase I, i.e. following ASTM G99 to collect sliding wear for the coatings produced. The 2 m wear track used a wear track radius of 8 mm, and the 100 m wear track length used a wear track radius of 10 mm. The ball was mild steel (Ø 7/32"; the pin load was 2 N; and the rotation speeds were 2.5 and 10.0 radians/sec (2 m and 100 m, respectively).

Figure 32a presents a typical 2 m wear track profile (friction as a function of wear length) for typical Zn-Ni alkaline (Dipsol) deposits produced using a PP electrical waveform. This illustrates that the deposit sliding wear profile remains relatively consistent throughout the 2 m length, but that there is some fluctuation over the duration of the test. The *mean* friction coefficient value is determined over the entire wear length; in this specific test, the mean was taken as 0.15. The values reported in Table 4 are the *averages* of the mean values obtained, i.e. testing three samples per coating. Figure 32b shows a typical 100 m track length wear profile (PP) indicating coating break-down and increase in friction coefficient.
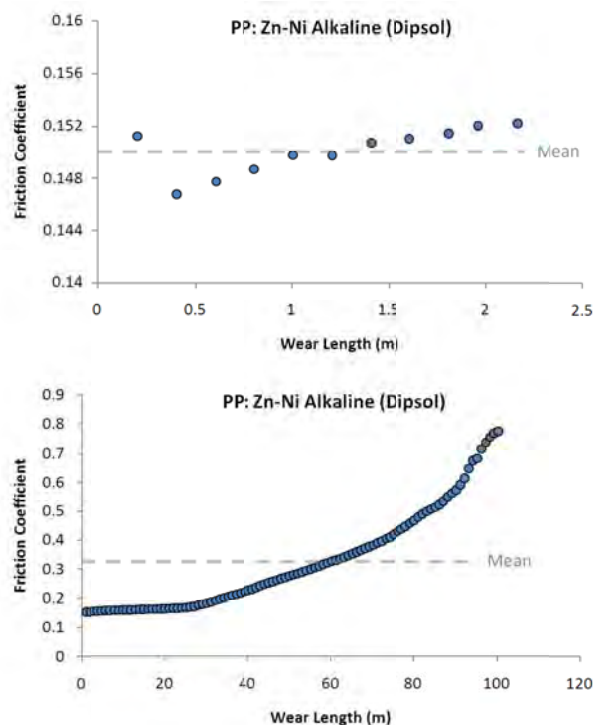

Figure 32: (a, left) 2 m pin-on-disc wear track profiles for a PP Zn-Ni deposit produced using the Dipsol alkaline bath. (b, right) 100 m pin-on-disc wear track profile for the PP deposit showing gradual increase.

10.2   TORQUE-TENSION ANALYSIS

In Phase I, the test procedure involved first installing and uninstalling the bolt 15 times and measuring the

resulting run-on and break-away torque. Run-on torque must be low enough such that installation machinery can torque the bolt to the necessary load; break-away torque must be high enough such that, while installed, the bolt does not come loose. The bolt was then visually inspected for any flaking or removal of coating, and if run-on and break-away values meet standards, are tested for 5 cycles of tightening to 30-60% of the UTS of the bolt to obtain a torque-tension relationship.

The same approach was taken in Phase II. The coefficient of friction was calculated using the following equation: $T = kDL$ [26], where T is the torque (inch-pounds), k is the friction coefficient, D is the diameter of the threaded part (taken as 0.5 inches), and L is the tension (pounds). Table 10 summarizes example measurements taken for Dipsol DC, PP, and PR samples, and Figure 33 summarizes their torque-tension profiles. This data illustrates that the deposits produced using different waveforms display more contrasting profiles, and that a clear difference exists between samples. Particularly, the values reported in Table 5 represent average values taken from a number of bolts, typically 3-5.

Table 10: Example torque-tension readings for Dipsol bath plating conditions.

| DC	Torque (inch-pounds)						Friction
Tension (pounds)	Trial 1	Trial 2	Trial 3	Trial 4	Trial 5	Average	k
4000	543	640	805	863	1006	771.4	0.3857
5000	685	732	883	969	1098	873.4	0.3494
6000	777	822	990	1078	1161	965.6	0.3219
7000	886	935	1080	1186	1229	1063.2	0.3038
8000	1001	999	1195	1272	1306	1154.6	0.2887
9000	1066	1082	1241	1455	1333	1235.4	0.2745
10,000	1136	1141	1351	1550	1491	1333.8	0.2668
11,000	1207	1249	1430	1609	1459	1390.8	0.2529
12,000	1320	1344	1518	1636	1539	1471.4	0.2452
						Average k:	**0.299**
PP	Torque (inch-pounds)						Friction
Tension (pounds)	Trial 1	Trial 2	Trial 3	Trial 4	Trial 5	Average	k
4000	337	368	362	325	400	358.4	0.1792
5000	395	429	425	417	468	426.8	0.1707
6000	454	484	493	479	542	490.4	0.1635
7000	527	536	561	516	595	547	0.1563
8000	581	585	603	619	646	606.8	0.1517
9000	639	653	675	570	700	647.4	0.1439
10,000	696	698	728	628	779	705.8	0.1412
11,000	757	787	786	840	843	802.6	0.1459
12,000	827	847	849	883	910	863.2	0.1439
						Average k:	**0.155**
PR	Torque (inch-pounds)						Friction
Tension (pounds)	Trial 1	Trial 2	Trial 3	Trial 4	Trial 5	Average	k
4000	283	375	456	416	434	392.8	0.1964
5000	405	457	527	481	511	476.2	0.1905
6000	456	507	597	545	601	541.2	0.1804
7000	535	569	666	608	664	608.4	0.1738
8000	592	678	716	696	727	681.8	0.1705
9000	667	692	787	762	809	743.4	0.1652
10,000	732	748	843	841	874	807.6	0.1615
11,000	779	818	911	890	931	865.8	0.1574
12,000	831	888	985	935	997	927.2	0.1545
						Average k:	**0.172**
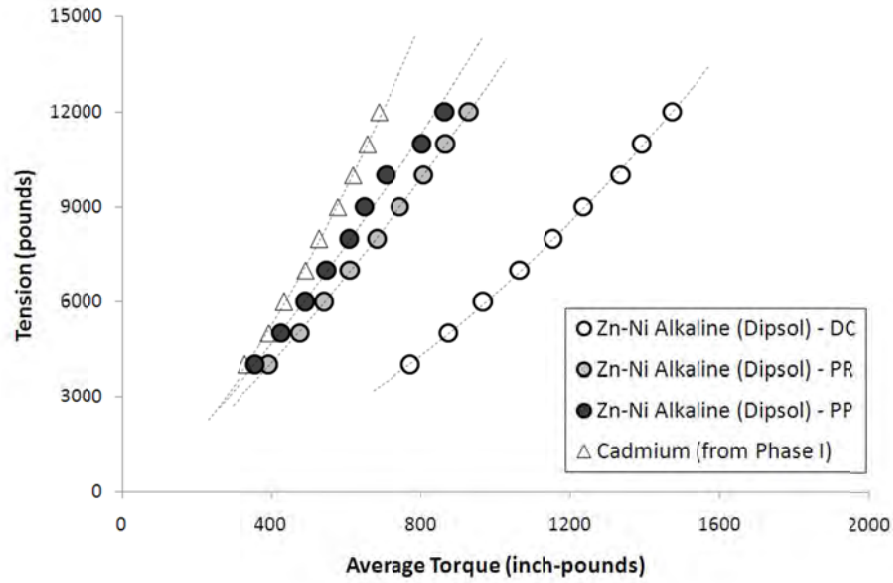
Figure 33: Torque-Tension data plot of tension versus average torque (from Table 10) for Zn-Ni alkaline deposits produced using the Dipsol chemistry. Deposits produced using pulsing electrical waveforms PP and PR appear to have a much lower friction coefficient under the range of values tested. Also shown is the profile for Cadmium obtained in Phase I.

11.0   REFERENCES

[1] M.J. Scoullos, G.H. Vonkeman, L. Thornton, Z. Makuch. "Chapter 4 – Cd" in: *Mercury, Cd, Lead – Handbook for sustainable heavy metals policy and regulation*, vol. 31. New York: Springer, 2001.

[2] Integrated Risk Information System, *Cd (CASRN 7440-43-9),* EnvFemental Protection Agency, 1998. Retrieved from web July 30th 2009. Available online at www.epa.gov/iris/subst/0141.htm.

[3] M. Bielawski, *Surface and Coatings Technology*, 179 (2004) 10.

[4] National Defense Center for Environmental Excellence (NDCEE), "Engineering and Technical Services for Joint Group on Pollution Prevention (JG-PP) Projects Joint Test Report BD-R-1-1 for Validation of Alternatives to Electrodeposited Cd for Corrosion Protection and Threaded Part Lubricity Applications", December 2002. Retrieved from web August 6th 2009. Available online at http://www.jgpp.com/projects/Cd/bisdsjtr/bisdsjtr.pdf.

[5] Joint Hard Chrome Alternatives Team (HCAT) and Joint Cadmium Alternative Team (JCAT). Summary notes from conference held 15-17 March 2005, Greensboro NC (May 16, 2005).

[6] NAVSEA Warfare Centers, "High Strength Steel Fastener Joint Test Protocol – for Validation of Alternatives to Electrodeposited Cadmium for High Strength Steel Fastener Applications", NSWCCD-SSES (March 17, 2004).

[7] www.asetsdefense.org/CdPlateAlternatives.aspx

[8] S. Gaydos, "Low Hydrogen Embrittling Alkaline Zinc-Nickel Plating for High Strength Steels", JCAT Program Review, Boeing – St. Louis (2006).

[9] S. Gaydos, "Evaluation of Dipsol IZ-C17 LHE Zinc-Nickel Plating", HCAT/JCAT Meeting, Boeing – St. Louis (August 14, 2007).

[10] S. Gaydos, "Status of LHE Zinc-Nickel Plating – A Cadmium Plating Alternative for the Aerospace Industry", IDS – Integrated Defense Systems, SUR/FIN 2007, Boeing – St. Louis (2007).

[11] E. Beck, "Joint Test Report for Execution of Phase I of 'High Strength Steel Joint Test Protocol for Validation of Alternatives to Low Hydrogen Embrittlement Cadmium for High Strength Steel Landing Gear and Component Application – of July 2003", US Navy Technical Report No. NAWCADPAX/TR-2006/164 (January 10, 2007).

[12] The Boeing Company, "High-Strength Steel Joint Test Protocol – For Validation of Alternatives to Low Hydrogen Embrittlement Cadmium for High-Strength Steel Landing Gear and Component Applications", Seattle WA (July 31, 2003).

[13] US 5,433,797 Nanocrystalline Metals
[14] EP 0670916 Nanocrystalline Metals
[15] US 5,352,266 Nanocrystalline Metals & Process of Producing the Same
[16] EP 1516076 Process for Electroplating metallic and metal matrix composite foils, coatings and microcomponents
[17] US 7320832 Fine-Grained Metallic Coatings Having the Coefficient of Thermal Expansion Matched to the one of the Substrate
[18] US 7,824,774 Fine-Grained Metallic Coatings Having the Coefficient of Thermal Expansion Matched to the one of the Substrate

[19] US 7,910,224 Fine-Grained Metallic Coatings Having the Coefficient of Thermal Expansion Matched to the one of the Substrate

[20] F. Altmayer, "Pulse and Periodic Reverse", Lesson 2: Basics in Electricity for Electroplaters in *Electroplating and Surface Finishing*, AESF Foundation and NASF, Inc, 2007.

[21] G. Palumbo, D.M. Doyle, A.M. El-Sherik, U. Erb, K.T. Aust, *Scripta Metall. Mater.*, 25 (1991) 679.

[22] D.M. Doyle, G. Palumbo, K.T. Aust, A.M. El-Sherik, U. Erb, *Acta Metall. Mater.*, 43 (1995) 3027.

[23] H. Natter, M.S. Loeffler, C.E. Krill, R. Hempelmann, *Scripta Mater.*, 44 (2001) 2321.

[24] D.A. Jones, Principles of Corrosion, 2nd Ed., Prentice Hall, Upper Saddle River (1996).

[25] R. Rofagha, U. Erb, D. Ostrander, G. Palumbo, and K.T. Aust, *Nanostructured Materials* 2 (1993) 1.

[26] D. Crotty, "Torque and Tension Control for Automotive Fasteners," *Metal Finishing* 9 (1999) 44.